

# INVESTIGATION OF TURBULENCE IN GRANULAR FLOW

by

Mohamed Abdelrahman

A thesis submitted to the faculty of  
The University of North Carolina at Charlotte  
in partial fulfillment of the requirements  
for the degree of Master of Science in  
Mechanical Engineering

Charlotte

2017

Approved by:

---

Dr. Russell Keanini

---

Dr. Alireza Tabarraei

---

Dr. Peter T. Tkacik

---

Dr. Yogendra Kakad



## ABSTRACT

MOHAMED ABDELRAHMAN. Investigation of turbulence in granular flow. (Under the direction of Dr. RUSSELL KEANINI)

Granular flow poses interesting questions in terms of both theoretical and applied mechanics. The increased utilization of vibrational finishing processes in the manufacturing of high precision components has resulted in an increased need to understand the behavior of granular fluids, particularly how granular fluids behave in vortex dominated turbulent flow. In this study, Particle Image Velocimetry (PIV) velocity data of various granular media flows are used to obtain the turbulence spectra. The turbulence spectra obtained for the various granular media are compared to the Kolmogorov turbulence spectrum observed in the flow of molecular liquids, to gain a greater understanding of how granular media behave in turbulent flow relative to the behavior of molecular liquids.

The turbulence spectra obtained in this study show that the granular media flows analyzed exhibited similar vortex breakdown and energy dissipation to what is normally observed in the turbulent flow of molecular liquids, therefore demonstrating that densely packed granular media behave similarly to molecular liquids when undergoing turbulent flow. These findings provide strong evidence to support the hypothesis that the observable random grain dynamics in densely packed grain media are equivalent to the unobservable random molecular dynamics present in the turbulent flow of molecular liquids.

## ACKNOWLEDGMENTS

I would like to thank my advisor, Dr. Russell Keanini for his continued guidance, support, and encouragement throughout my graduate study. I would also like to thank Dr. Peter Tkacik, Dr. Yogendra Kakad, and Dr. Alireza Tabarraei for taking the time to serve on my thesis committee and providing me valuable feedback.

I would also like to thank my parents and my brother for their continued encouragement and support throughout my graduate study.

Finally, I would like to thank Mr. Hussien Shahinian, Mr. Kapil Gaur, and Mr. Tony Martin for their help and support on this project.

My best wishes to the faculty and fellow graduate students at the University of North Carolina at Charlotte College of Engineering.

## TABLE OF CONTENTS

LIST OF TABLES .....	vi
LIST OF FIGURES .....	vii
CHAPTER 1: VIBRATORY FINISHING.....	1
CHAPTER 2: UNDERSTANDING GRANULAR FLOW .....	3
2.1: Gas-like Granular Flow .....	4
2.2: Liquid-like Granular Flow .....	6
CHAPTER 3: KEY POINTS ADRESSED IN THESIS .....	8
CHAPTER 4: EXPERIMENTAL SYSTEM.....	9
CHAPTER 5: ANALYSIS OF RANDOM GRAIN DYNAMICS.....	11
5.1: Kolmogorov's Theory of Turbulence .....	11
5.2: Alternative Method for Finding the Turbulence Spectrum.....	15
CHAPTER 6: GRANULAR FLOW TURBULENCE SPECTRUM.....	18
CHAPTER 7: CONCLUSIONS .....	45
REFERENCES .....	46
APPENDIX A: OVERVIEW OF MATLAB CODE.....	48
APPENDIX B: MAIN FILE.....	49
APPENDIX C: RAW2UVQM FUNCTION .....	75
APPENDIX D: FFT_SETUP FUNCTION .....	77
APPENDIX E: VIBRATIONREMOVE FUNCTION .....	79
APPENDIX F: PSD FUNCTION.....	82
APPENDIX G: PSDP FUNCTION .....	84

LIST OF TABLES

Table 1: Grain Media Specifications ..... 19

Table 2: Grain Media Specifications ..... 20

Table 3: Grain Media Specifications ..... 21

## LIST OF FIGURES

Figure 1: Diagram of Experimental Apparatus.....	2
Figure 2: Vibratory Finishing System .....	9
Figure 3: PIV Velocity Vector Map .....	10
Figure 4: Kolmogorov's Turbulence Spectrum .....	13
Figure 5: Turbulence spectrum of liquid metal flow generated using varying magnetic field frequencies .....	16
Figure 6: The PSD of the v velocity component for the H-10-08 media.....	22
Figure 7:The PSD of the u velocity component for the H-10-08 media.....	23
Figure 8: The PSD of the v velocity component for the RCP 0909 media.....	24
Figure 9:The PSD of the u velocity component for the RCP 0909 media.....	25
Figure 10:The PSD of the v velocity component for the 2mm sphere media.....	26
Figure 11: The PSD of the u velocity component for the 2mm sphere media.....	27
Figure 12: The PSD of the v velocity component for the 2mm sphere media under higher amplitude vibration. ....	28
Figure 13: The PSD of the u velocity component for the 2mm sphere media under higher amplitude vibration. ....	29
Figure 14: The PSD of the v velocity component for the RS 19K media. ....	30
Figure 15: The PSD of the u velocity component for the RS 19K media. ....	31
Figure 16: The PSD of the v velocity component for the mixed media. ....	32
Figure 17: The PSD of the u velocity component for the mixed media. ....	33
Figure 18:The PSD of the v velocity component for the RS 1022 ZS media.....	34
Figure 19: The PSD of the u velocity component for the RS 1022 ZS media.....	35
Figure 20: The PSD of the v velocity component for the RSG 10/10 S media. ....	36

Figure 21: The PSD of the u velocity component for the RSG 10/10 S media. ....	37
Figure 22: The PSD of the v velocity component for the RS 35/15 DZS media.....	38
Figure 23: The PSD of the u velocity component for the RS 35/15 DZS media.....	39
Figure 24: The PSD of the v velocity component for the RS 10/10 media. ....	40
Figure 25: The PSD of the u velocity component for the RS 10/10 media. ....	41
Figure 26: The PSD of the v velocity component for the 2050 40/13 DZ media.....	42
Figure 27: The PSD of the u velocity component for the 2050 40/13 DZ media.....	43



## CHAPTER 1: VIBRATORY FINISHING

Vibratory finishing processes are utilized to deburr and provide the desired surface finish for metallic components in a wide variety of industries. The vibratory finishing process, depicted in Figure 1, involves placing small grains, referred to as grain media in this study, along with a compound such as water or other chemical mixtures, and the metallic workpieces in an open container [1]. The container is placed on springs that are connected to an unbalanced motor [1]. During processing, the motor causes the container to vibrate, and the resulting vibration produces fluid-like motion of the grain media placed inside the container [1]. The movement of the media, as well as the impact between the media and the work pieces produces the desired deburring and surface finish improvement in the work piece [1]. Processing time, as well as media and compound selection are dependent on the desired surface finish quality [1].

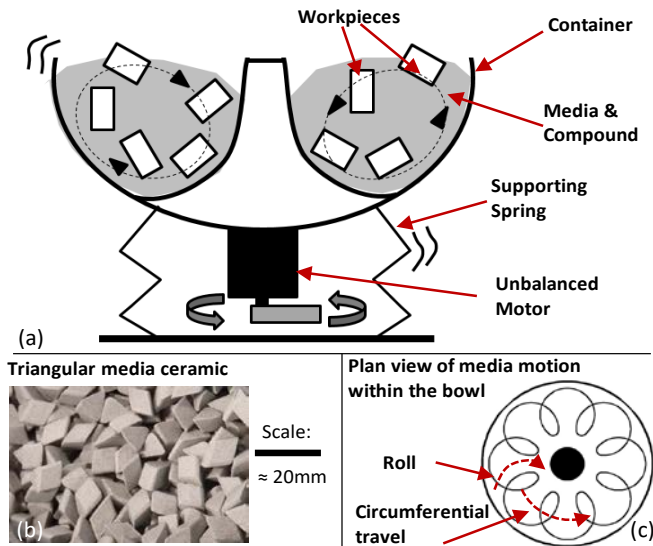


Figure 1: Diagram of Experimental Apparatus [1]  
 (a) Schematic of a vibratory finishing apparatus, (b) sample of grain media, (c) grain media motion from top view [1].

The research efforts undertaken by the vibratory finishing research group at the University of North Carolina at Charlotte to better understand the fluid-like motion of grain media during vibratory finishing processes and how it affects material removal have also raised an important question of grain media behavior in vortex dominated turbulent flow, specifically how grain media behave under turbulent flow conditions relative to the behavior of molecular liquids.

The question of grain media behavior in vortex dominated turbulent flow is the major question being addressed in this thesis. In the next chapters, this report will cover the different ways of modeling grain media flow, as well as discuss the procedures used to obtain the velocity data and analyze the turbulent flow properties of grain media. The report will use the generated data to answer the question of how grain media behave under turbulent flow conditions relative to the behavior of molecular liquids.

## CHAPTER 2: UNDERSTANDING GRANULAR FLOW

Studying the flow of granular media poses a different set of challenges than what is usually encountered when studying molecular liquid flow. For instance, granular media are macroscopic, therefore they experience dissipative interactions which cause the kinetic energy of the grains' centers of masses to be dissipated as heat when grains collide [2]. Another major distinction is that the mass of the average grain is of the order of  $10^{20}$  molecular masses, therefore the kinetic or potential energy of a grain is orders of magnitude larger than molecular thermal energy, and the temperature of the environment can be considered negligible when modeling granular flow [2].

Various researchers in the past have attempted to gain a greater understanding of the properties of granular flow by modeling granular flow relative to the models of a more well understood flow, such as the flow of gases or liquids. One of the researchers that studied different models of granular flow extensively was Andrea Puglisi. In Chapter 2 of his book, *Transport and Fluctuations in Granular flow*, Puglisi discussed modeling granular flow as a gas of inelastic hard spheres.

## 2.1: Gas-like Granular Flow

In granular flow modeled as a flow of inelastic hard spheres, particles collide dissipating their energy in the form of heat [3]. This process acts to conserve momentum, maintaining the velocity of the center of mass of the individual grains unchanged [3]. Modeling granular flow as a flow of a gas of inelastic hard spheres utilizes the Boltzmann equation with the assumption of molecular chaos [3].

The Boltzmann equation is used to describe the statistical behavior of a thermodynamic system in a non-equilibrium state [3]. The Boltzmann equation is most widely used to model the change of a macroscopic quantity, such as energy or particle number in particle transporting fluids or gases [3]. More information regarding the Boltzmann theory and how it is derived for this particular model can be found in chapter 2 of Puglisi's book in reference 3.

In order to use the Boltzmann equation, molecular chaos must be assumed in the flow [3]. This assumption states that colliding particles in the flow are assumed to be uncorrelated prior to the collision [3]. The assumption of molecular chaos utilizes the Boltzmann-Grad limit [3]. The Boltzmann-Grad limit states that in a rarefied gas, in which the number of particles is very large, change of position of any specific particle is very small, and the volume occupied by the particles is very small, the chance of a collision between any two selected particles can be considered a rare event [3].

Modeling granular flow as a flow of a gas of hard inelastic spheres has been of great benefit to researchers attempting to gain a greater understanding of the properties of

granular flow, but the model is not without limitations, with one problem in particular referred to as the problem of inelastic collapse [3].

The problem of inelastic collapse occurs when granular flows are modeled as inelastic collisions with a fixed restitution coefficient [3]. A simple example where this problem can be observed is when modeling three particles on a line, with the outer particles moving closer to each other, and the particle in the middle bouncing between them [3]. When the flow is modeled with a fixed restitution coefficient, the cycle of collisions repeats endlessly, and result in an infinite number of collisions occurring in a finite time [3]. In order for inelastic collapse to occur under this model, the collision needs to include more than three particles, with the number of particles required increasing as the restitution coefficient increases towards 1 [3]. Due to this problem, and other limitations, researchers studying granular flow began working to develop more durable models that accurately depict the properties of granular flow. One such model is the model of granular hydrodynamics [3].

## 2.2: Liquid-like Granular Flow

In chapter three of his book, *Transport and Fluctuations in Granular Fluids*, Puglisi introduced the Granular Kinetic Theory, which can be used to model granular fluids in a non-equilibrium state. The theory introduced in Puglisi's book applies as long as the non-homogeneity in the flow satisfies the small gradients criterion. Puglisi's book also introduced the Chapman-Enskog procedure, which introduced the key steps necessary to obtain a non-homogenous solution of the Boltzmann equation in the presence of weak gradients [4].

The modeling of granular flow as liquid like flow was a major achievement that has inspired researchers to study granular flow and its properties as it relates to the governing principles of fluid flow, in the hope of gaining a greater understanding of the properties of granular flow.

One of the major research projects that aimed to investigate the properties of granular flow and the physical correspondence between macroscopic grain structures and the molecular liquid systems, was a study conducted at the Mechanical Engineering department at the University of North Carolina at Charlotte by Dr. R Keaninni, Dr. B Mullaney, and Dr. P Thacik. The study titled: *Application of particle image velocimetry (PIV) to vibrational finishing*, investigated the properties of granular flow by obtaining Particle Image Velocimetry (PIV) velocity data of the flowing media [1]. This study was one of the first studies conducted that studied granular flow as a continuous flow, and the findings of this study provided the inspiration for this thesis research to further

investigate turbulent granular flow, and understand the behavior of granular flow in a vortex dominated turbulent flow.

### CHAPTER 3: KEY POINTS ADRESSED IN THESIS

From the findings of the study conducted by Dr. R Keanini, Dr. P Thacik, and Dr. B Mullaney in reference 1, we possess strong evidence that macroscopic vibrated grain media represent analogs of molecular liquids. Building upon the theoretical findings mentioned in chapter 2 of this thesis, as well as the experimental results obtained by the Vibratory finishing research group at the University of North Carolina at Charlotte, it can be argued that the directly observed random grain motion occurs at the unobservable molecular scales as well.

This study takes advantage of the physical correspondence between macroscopic grain structures and molecular liquid systems to investigate random grain dynamics, and gain a greater understanding of the behavior of grain media under turbulent flow conditions as it relates to the behavior of molecular liquids. The findings of this study will provide the evidence necessary to determine whether the properties of the observable random grain motion are equivalent to the properties of the molecular scale motion of molecular liquids under turbulent flow conditions.



## CHAPTER 4: EXPERIMENTAL SYSTEM

The experimental system used to obtain the velocity data analyzed in this study presented in Figure 2, consisted of a vibratory bowl, a Redlake camera (Motionextra HG-XR) to capture images at a rate of 500 frames per second (fps), a halogen lamp (ARRI EB 400/575 D) to provide sufficient illumination to the imaged region [1].

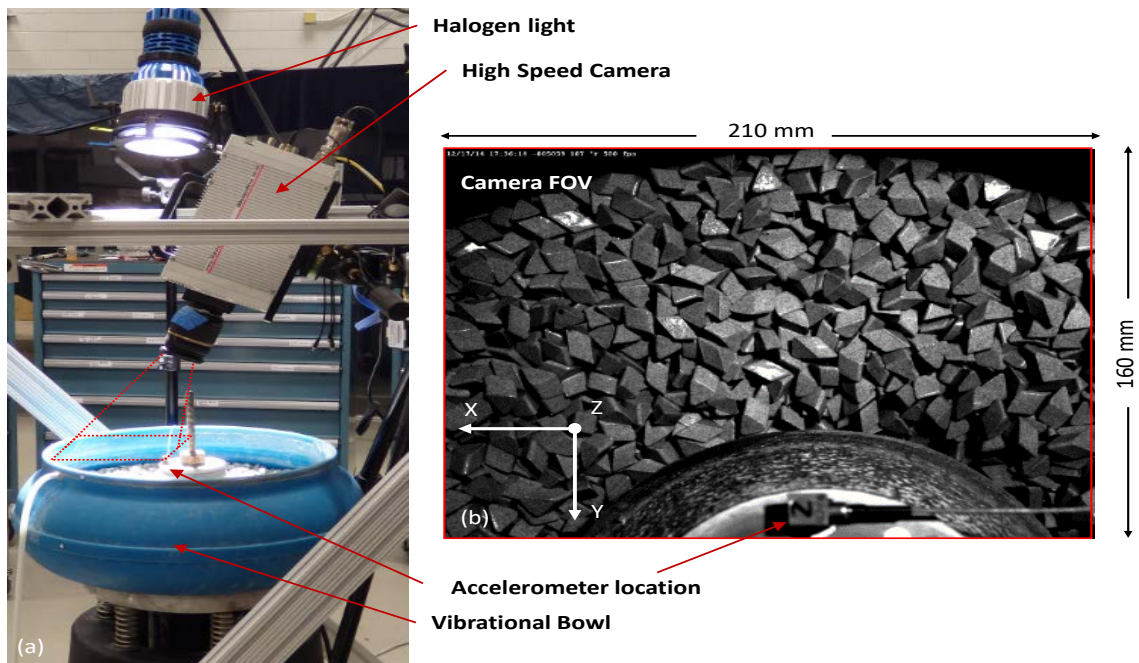


Figure 2: Vibratory Finishing System [1]  
(a) Experimental Setup, (b) Camera field of view [1]

For each test conducted during the study, 5060 frames were captured, corresponding to 10.12 seconds [1]. The collected data was then uploaded to the Dantec Dynamics™ DynamicStudio (2013) PIV software, which processes the data, resulting in 5059 vector fields for each experimental run [1]. An example of the obtained vector field spectrum is presented in Figure 3 [1]. More details regarding the experimental setup and the PIV data analysis can be found by reviewing the Applications of PIV to Vibratory Finishing study in reference 1.

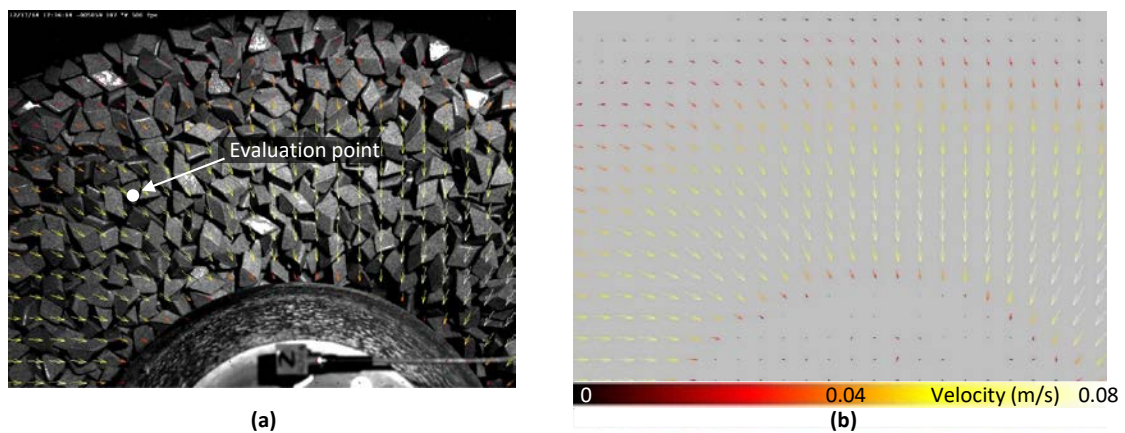


Figure 3: PIV Velocity Vector Map [1]  
(a) Velocity vector map placed on an image of the test. (b) Vector map as outputted by the PIV software [1]

## CHAPTER 5: ANALYSIS OF RANDOM GRAIN DYNAMICS

### 5.1: Kolmogorov's Theory of Turbulence

Turbulent flow can be modeled as consisting of vortices or eddies as referred to in Kolmogorov's theory [5]. Each eddy present in the flow is considered to be localized over a region of size  $l$ , and is considered to be homogenous over its localized region [5]. Under turbulent flow conditions, an energy cascade exists where energy is transferred from larger vortices or eddies to smaller and smaller vortices [5]. This cascade continues until the localized Reynolds number associated with the specific length scale is sufficiently low that it is unable to support the motion of vortices [5].

The theory of turbulence developed by Kolmogorov in 1941, describes the energy transfer between larger and smaller eddies in a turbulent flow. The theory also describes the amount of energy contained within the various eddy sizes present in the flow. The theory utilizes two important length scales: the energy containing scale, and the dissipation scale [5].

The three main principles used in Kolmogorov's theory to explain the behavior of vortices in turbulent flow are Kolmogorov's hypothesis of local isotropy, Kolmogorov's first similarity hypothesis, and Kolmogorov's second similarity hypothesis [5].

Kolmogorov's hypothesis of local isotropy states that for homogenous turbulence, the turbulent kinetic energy should remain invariant as the interrogation area in the flow varies [5]. The hypothesis also states that the behavior of small-scale vortices remains the same in all directions of the flow [5]. According to Kolmogorov, this behavior occurs due to the fact that variations in the flow in large scale vortices become unobservable as larger vortices begin to break down and transfer their energy to smaller vortices, therefore resulting in statistically isotropic small-scale turbulent motion [5].

Kolmogorov's first similarity hypothesis states that as energy is passed from larger to increasingly smaller vortices, directional variations and geometrical variations are lost [5]. The result of this principle is that the statistics of small-scale motions can be considered to be of a universal form independent of the mean flow field [5]. The behavior of these small-scale vortices is therefore only dependent on inertial forces and kinematic viscosity [5].

Kolmogorov's second similarity hypothesis states that for intermediate scale vortices, since the Reynolds number is relatively high, the flow properties will not be affected by the kinematic viscosity, therefore the universal form that defines intermediate-scale vortices is dependent only on inertial forces and independent of the kinematic viscosity [5].

From the first and second similarity hypotheses, it can be determined that the flow beyond the energy containing scale can be divided into two regions: the inertial subrange (intermediate-scale vortices) where the motion is determined only by inertial forces independently of viscous effects, and the dissipation range (small-scale vortices), where

the motion of vortices is determined by both inertial and viscous effects [5]. The energy spectrum developed by Kolmogorov depicting the energy transfer cascade in turbulent flow is presented in Figure 4 [6].

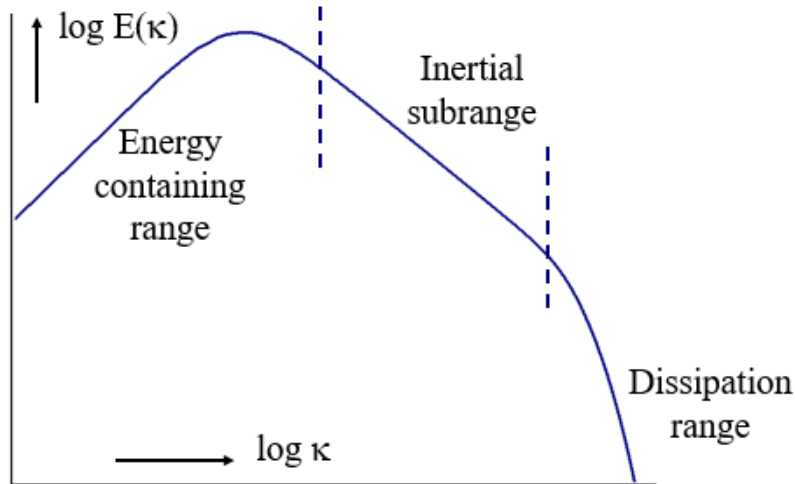


Figure 4: Kolmogorov's Turbulence Spectrum [6]  
 $E(k)$  is the Kinetic Energy and  $k$  is the wave number [6]

Figure 4 captures the energy transfer cascade by plotting the kinetic energy measured at different wave numbers. Wave numbers represent the number of waves present in a unit distance, which in our case correlates with the number of vortices present in any given location in the flow field. In this analysis, wave numbers can be used to represent the size of the vortices present in the flow, with higher wave numbers correlating with smaller vortices. From the energy spectrum presented in Figure 4, it can be seen that kinetic energy decreases at larger wave numbers, therefore demonstrating that kinetic energy in turbulent flow is dissipated from larger vortices to increasingly smaller vortices [5].

For the purposes of this study, the report will focus only on the inertial subrange, where the characteristic Kolmogorov  $-5/3$  slope is present, and where the vortices in the granular flow analyzed for this study are observable. Within the inertial subrange, the Kinetic Energy  $E(k)$  is calculated using Equation 1[5].

$$E(k) = C \varepsilon^{\frac{2}{3}} k^{-\frac{5}{3}} \quad (1)$$

Where  $C$  is the Kolmogorov constant, experimentally determined to be 1.5,  $\varepsilon$  is the dissipation, and  $k$  is the wave number [5]. For a more in depth overview of the equation and it's derivation review the work of Karima Khusnutdinova in reference 5.

In this study, the obtained velocity data were not spatially filtered, instead the obtained velocity data were filtered using a Fourier Transform in the time domain, therefore it was not possible to obtain turbulence spectra based on kinetic energy and wave numbers. Due to the type of data obtained, an alternative method was needed to obtain the turbulence spectra and evaluate kinetic energy variation between larger and smaller vortices utilizing the available time domain data. The next section discusses in detail the alternative method utilized to obtain the turbulence spectra, as well as a previous study that utilized this method effectively to obtain the turbulence spectra of the flow of a molecular liquid, therefore demonstrating the applicability of this method to evaluating turbulent flow.

## 5.2: Alternative Method for Finding the Turbulence Spectrum

In this study, obtaining the energy spectrum by obtaining the kinetic energy at different wave numbers proved challenging since the velocity data used in this study were obtained using a Fourier transform in the time domain, therefore an alternative method was needed to obtain the turbulence spectrum.

In the research article, *The Study of Turbulence in MHD Flow Generated by Rotating and Travelling Magnetic Fields* in reference 7, the researchers obtained the turbulence spectrum by calculating the Power Spectral Density (PSD) of the velocity components and plotting the PSD vs. the frequency [7]. The PSD of a signal over a specific frequency band produces the average power of the signal over that frequency, generating the turbulence spectrum presented in Figure 5 [9][7].

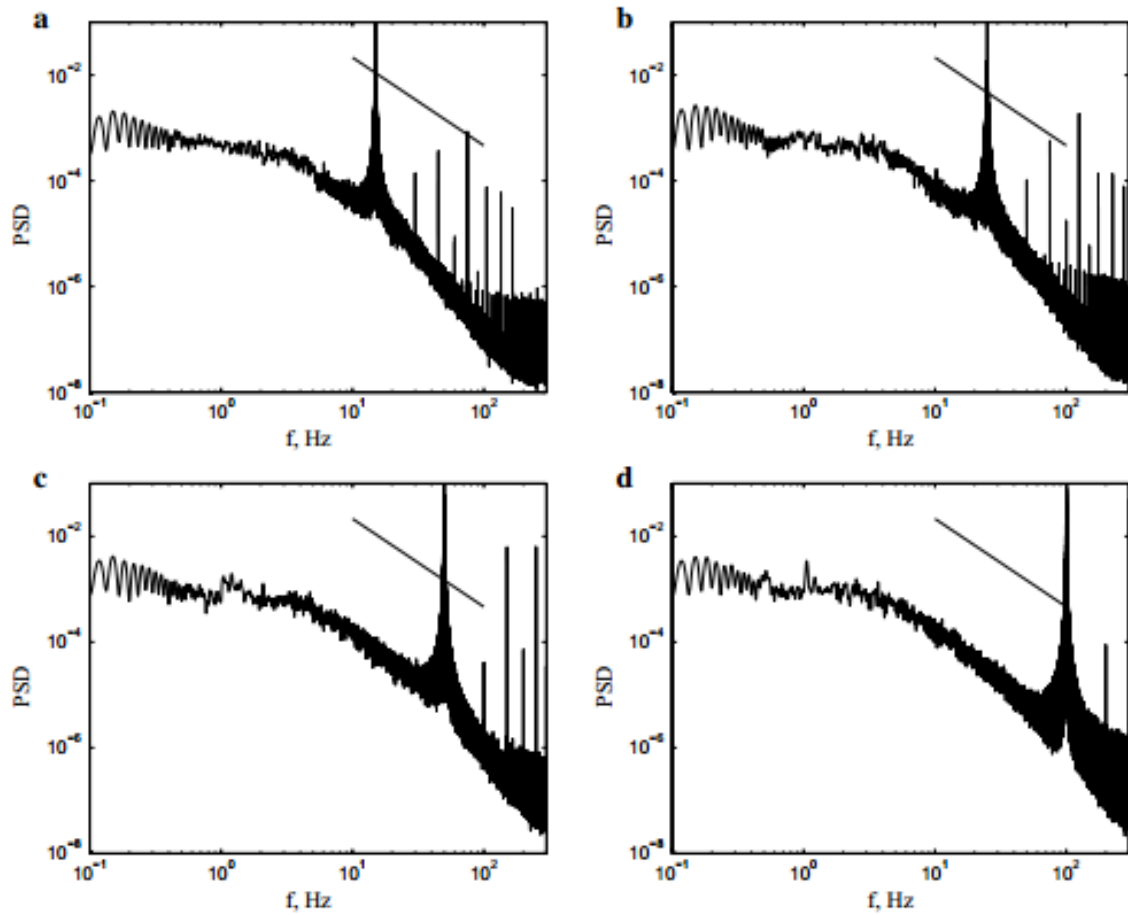


Figure 5: Turbulence spectrum of liquid metal flow generated using varying magnetic field frequencies [7]

a: 15 Hz, b: 25 Hz, c: 50 Hz, d: 100 Hz. [7]

In the spectrum presented in Figure 5, the frequency represents the number of waves passing a point in a certain time, with higher frequencies correlating with smaller vortices. Therefore, this method can be used to depict the amount of kinetic energy present in the different size vortices within the flow by calculating the velocity associated with each frequency range.



From the plot in Figure 5, it can also be seen that the obtained turbulence spectrum matched the slope of the Kolmogorov spectrum for the inertial subrange region, therefore proving that this method can be utilized to obtain accurate and repeatable turbulence spectra.

## CHAPTER 6: GRANULAR FLOW TURBULENCE SPECTRUM

The turbulence spectra in this study were obtained using the PSD vs. frequency approach to capture how the kinetic energy of the flowing media varies with the different sized vortices present in the flow. The spectra were obtained for the 10 types of media included in the study, and the obtained turbulence spectra for each media type are arranged based on the measured packing density, from highest density to lowest density. The types of media included in the study are listed in Tables 1 through 3, along with their dimensions, packing densities, materials, and area.

Table 1: Grain Media Specifications





	Image	Material	Packing Density (kg/m <sup>3</sup> )	Dimensions (mm)	Area (m <sup>2</sup> )
H-10-08		Plastic	2033	9 x 6 x 8	0.000236
RCP 09/09		Ceramic	2033	9 x 9	0.000284
2mm Spheres		Composite	1748	N/A	0.0000126
RS 19K		Ceramic	1711	19	0.00287

Table 2: Grain Media Specifications







Grain Media	Image	Material	Packing Density (kg/m <sup>3</sup> )	Dimensions (mm)	Area (m <sup>2</sup> )
Mixed Media		Composite	1615	N/A	0.00968
RS 10/22 ZS		Ceramic	1600	10 x 20	0.000785
RSG 10/10 S		Ceramic	1390	10 x 10	0.00035
RS 35/15 DZS		Ceramic	1285	35 x 15	0.0021

Table 3: Grain Media Specifications

Grain Media	Image	Material	Packing Density (kg/m <sup>3</sup> )	Dimensions (mm)	Area (m <sup>2</sup> )
RS10/10		Ceramic	1147	10 x 10	0.00035
2050 40/13 DZ		Plastic	752	36 x 13	0.00205

The turbulence spectra obtained for the grain media in Tables 1,2, and 3 are arranged in Figures 6 through 27.

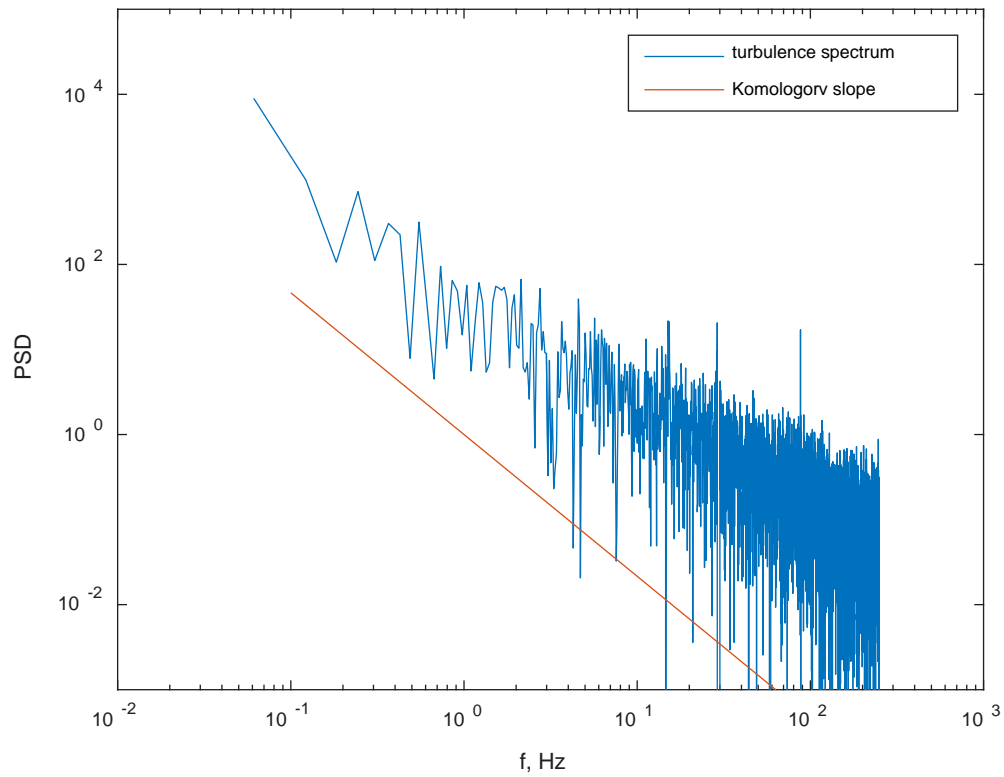


Figure 6: The PSD of the v velocity component for the H-10-08 media. The solid line represents the Kolmogorov  $-5/3$  slope

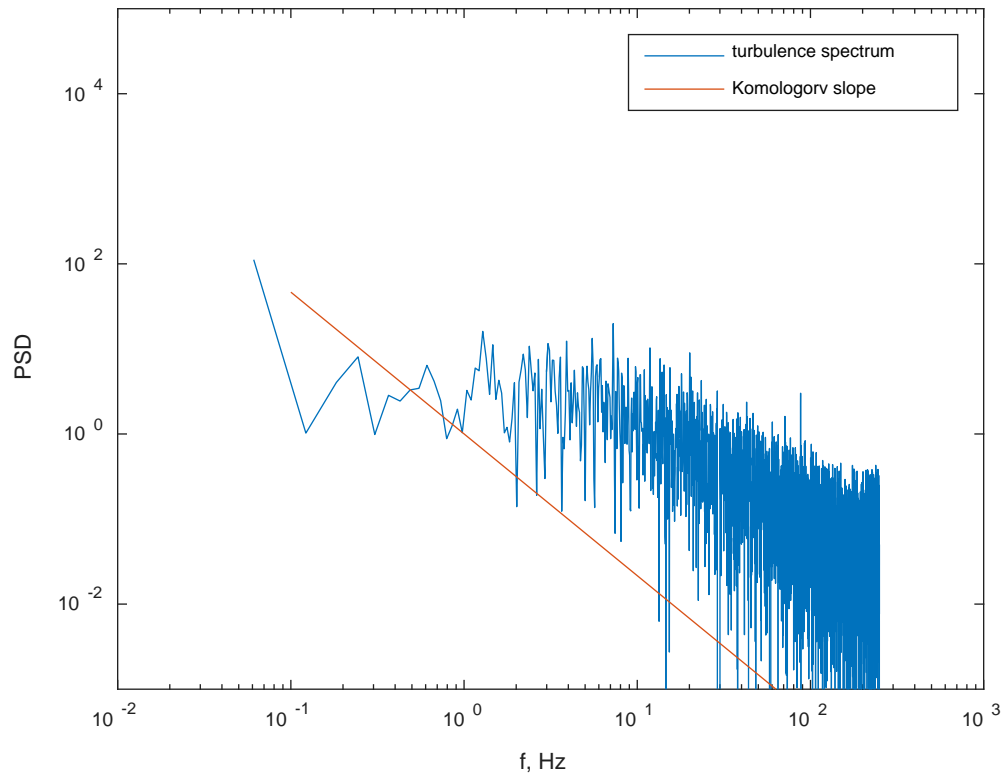


Figure 7: The PSD of the u velocity component for the H-10-08 media. The solid line represents the Kolmogorov  $-5/3$  slope

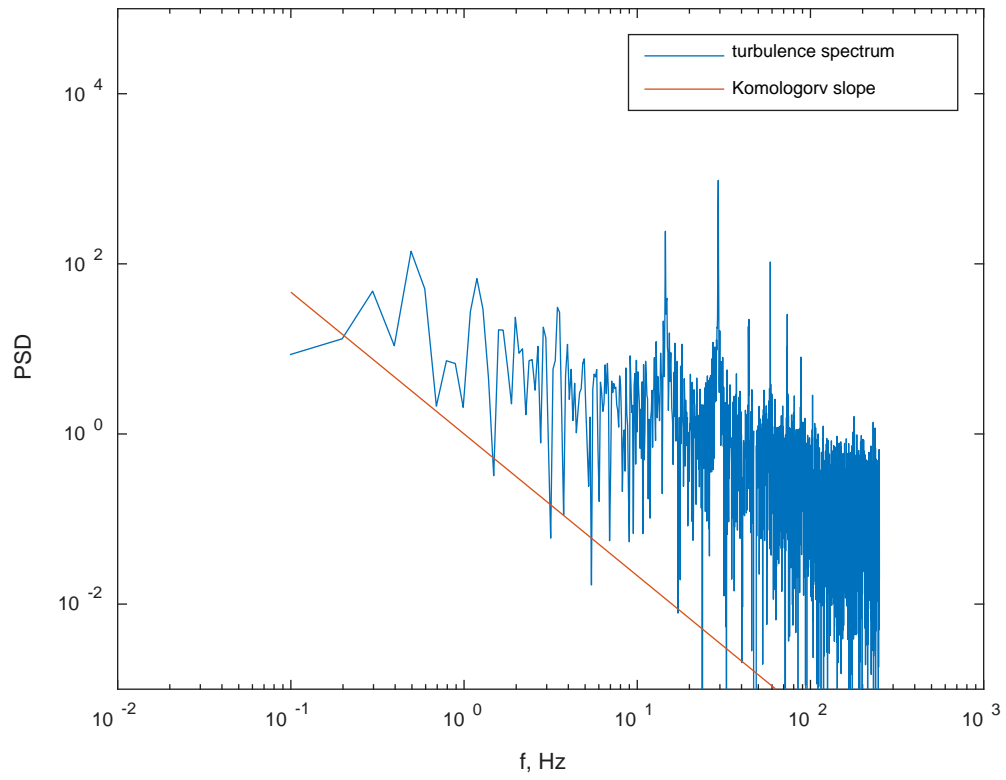


Figure 8: The PSD of the  $v$  velocity component for the RCP 0909 media. The solid line represents the Kolmogorov  $-5/3$  slope



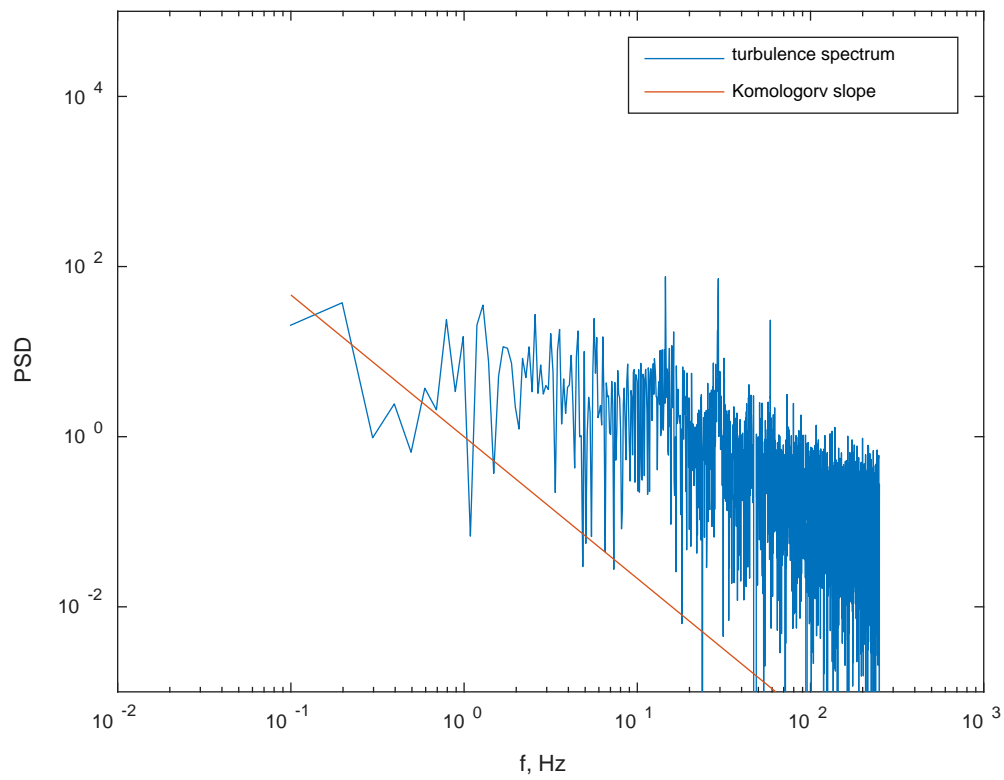


Figure 9: The PSD of the u velocity component for the RCP 0909 media. The solid line represents the Kolmogorov  $-5/3$  slope

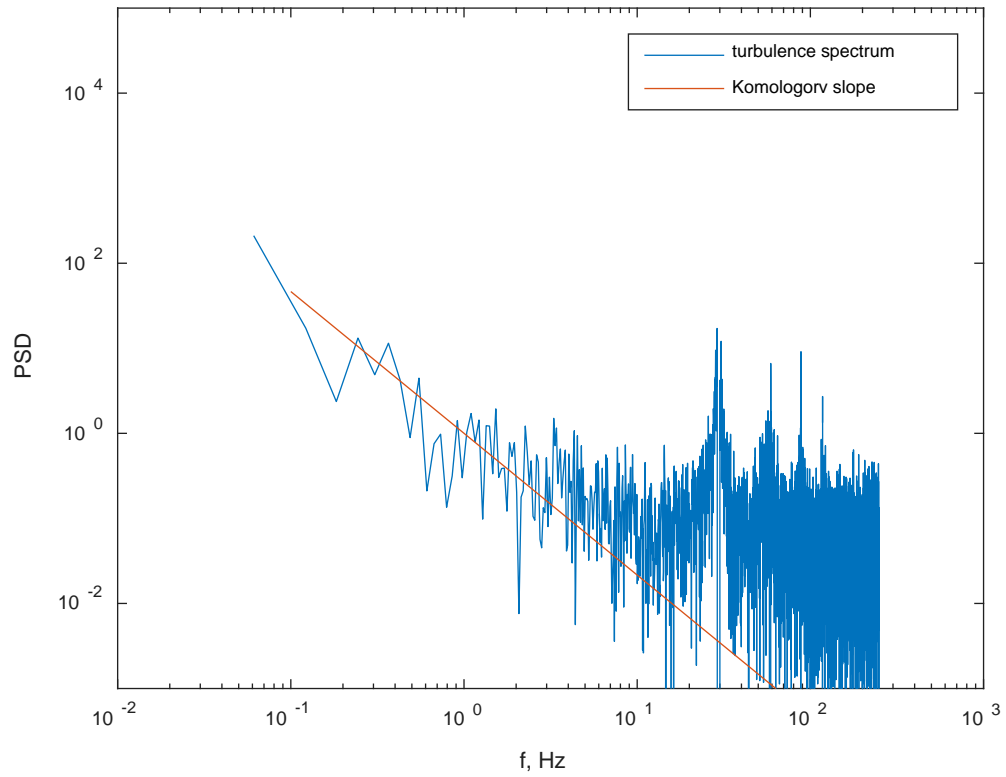


Figure 10: The PSD of the  $v$  velocity component for the 2mm sphere media. The solid line represents the Kolmogorov  $-5/3$  slope

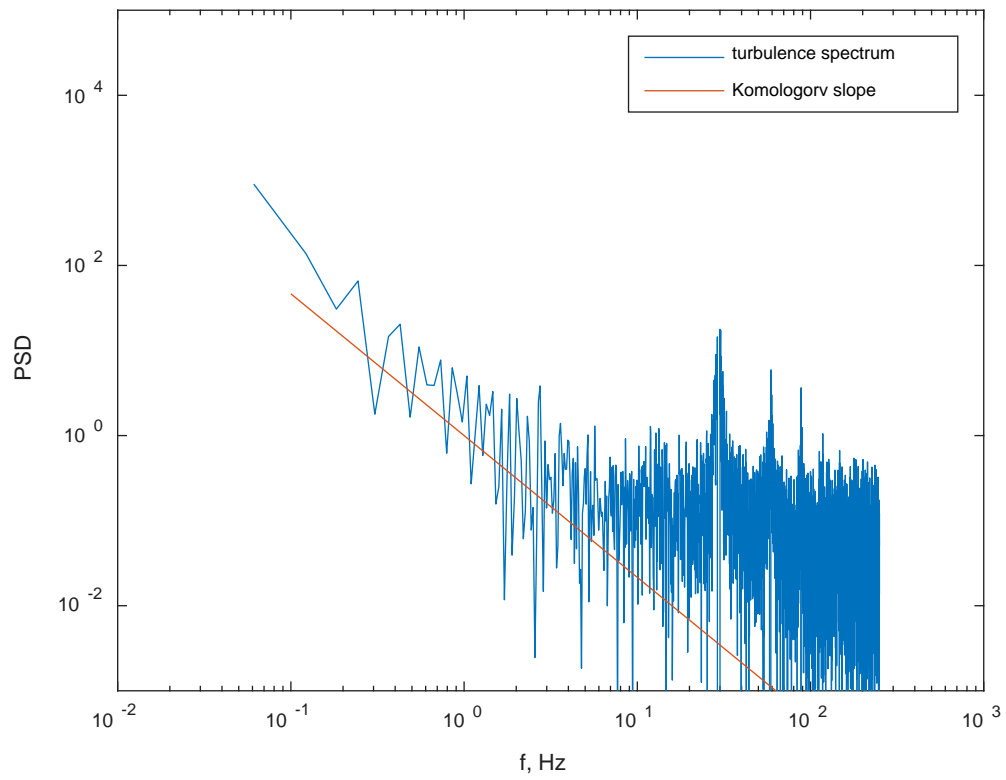


Figure 11: The PSD of the u velocity component for the 2mm sphere media. The solid line represents the Kolmogorov  $-5/3$  slope

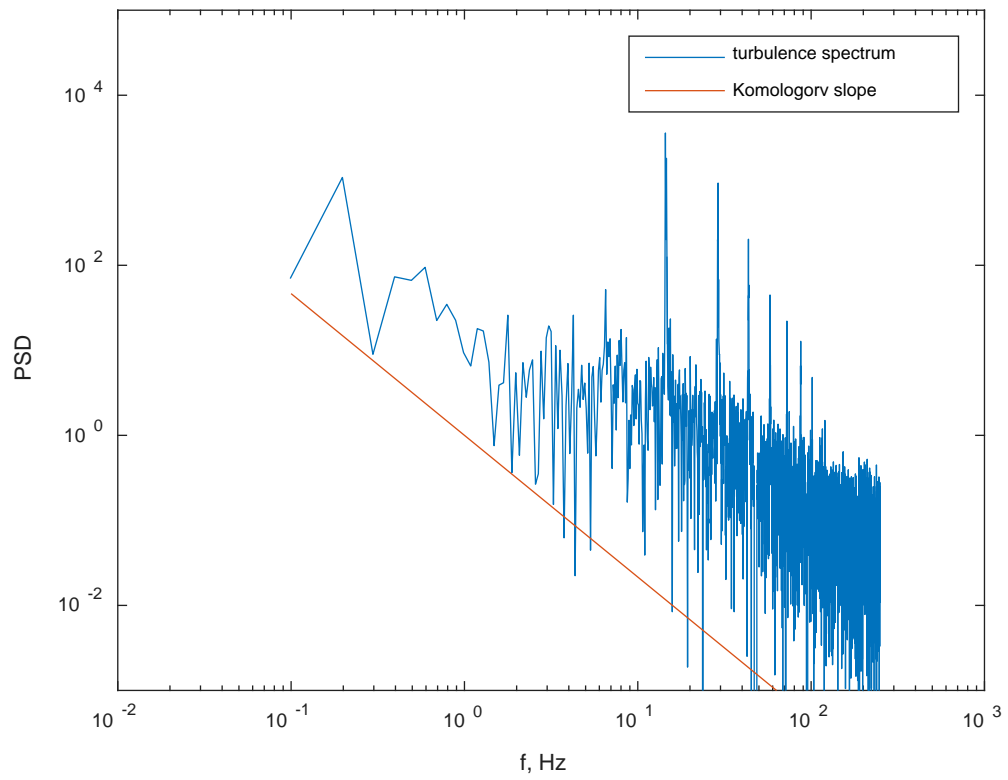


Figure 12: The PSD of the v velocity component for the 2mm sphere media under higher amplitude vibration.  
The solid line represents the Kolmogorov  $-5/3$  slope

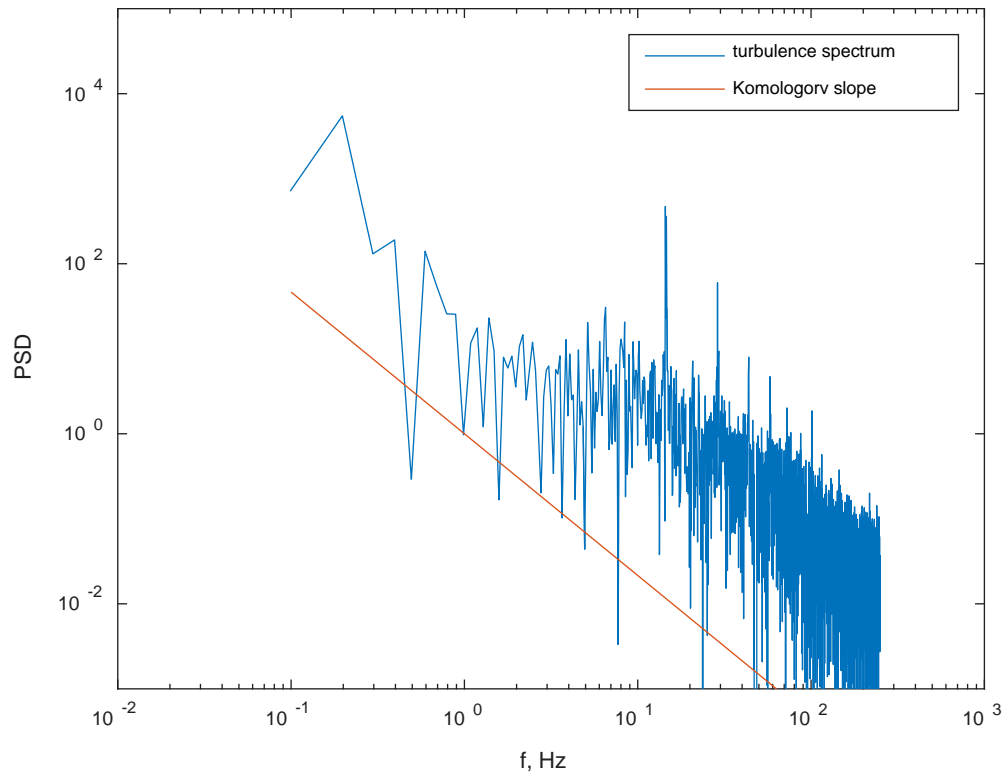


Figure 13: The PSD of the u velocity component for the 2mm sphere media under higher amplitude vibration.  
The solid line represents the Kolmogorov  $-5/3$  slope

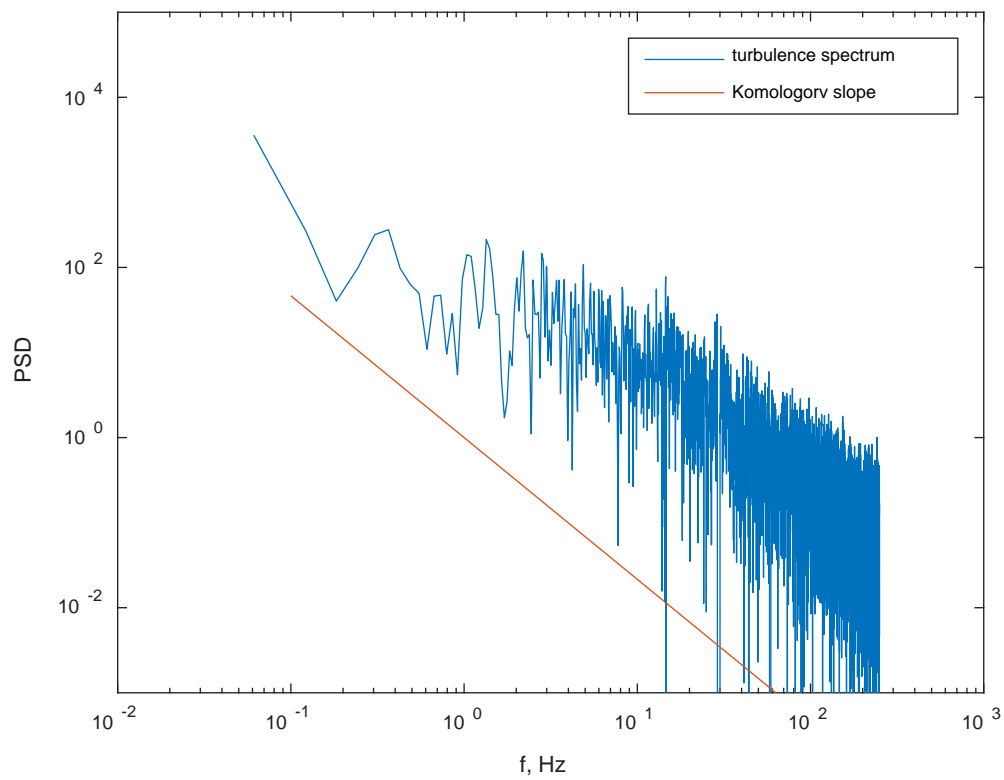


Figure 14: The PSD of the v velocity component for the RS 19K media. The solid line represents the Kolmogorov  $-5/3$  slope

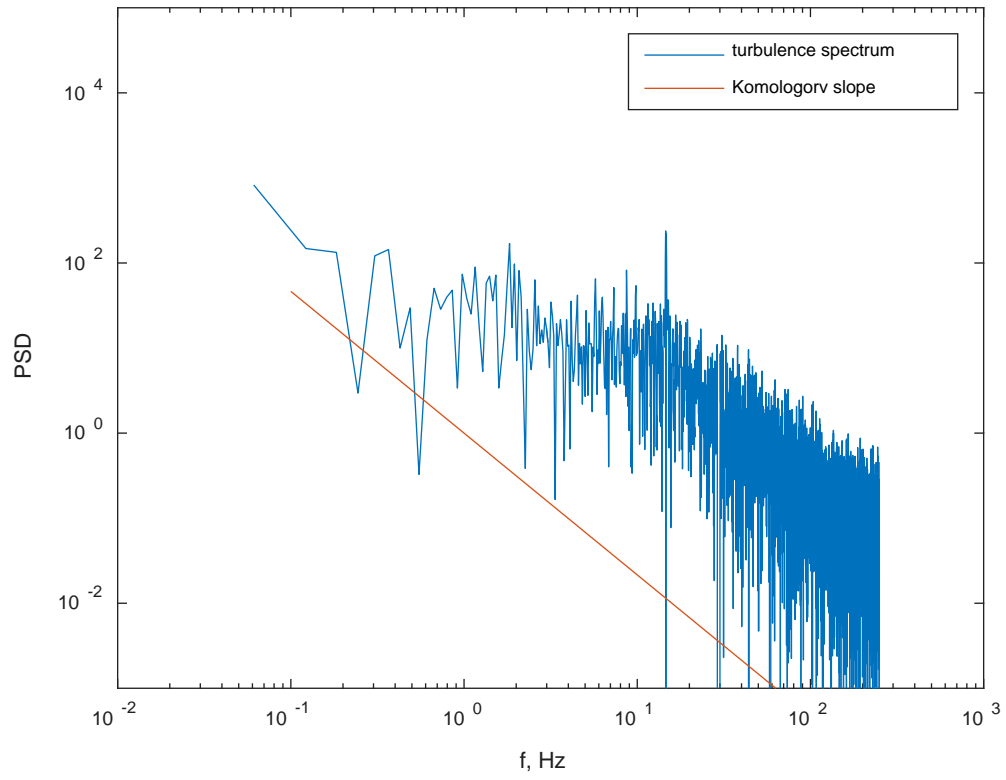


Figure 15: The PSD of the u velocity component for the RS 19K media.  
The solid line represents the Kolmogorov  $-5/3$  slope

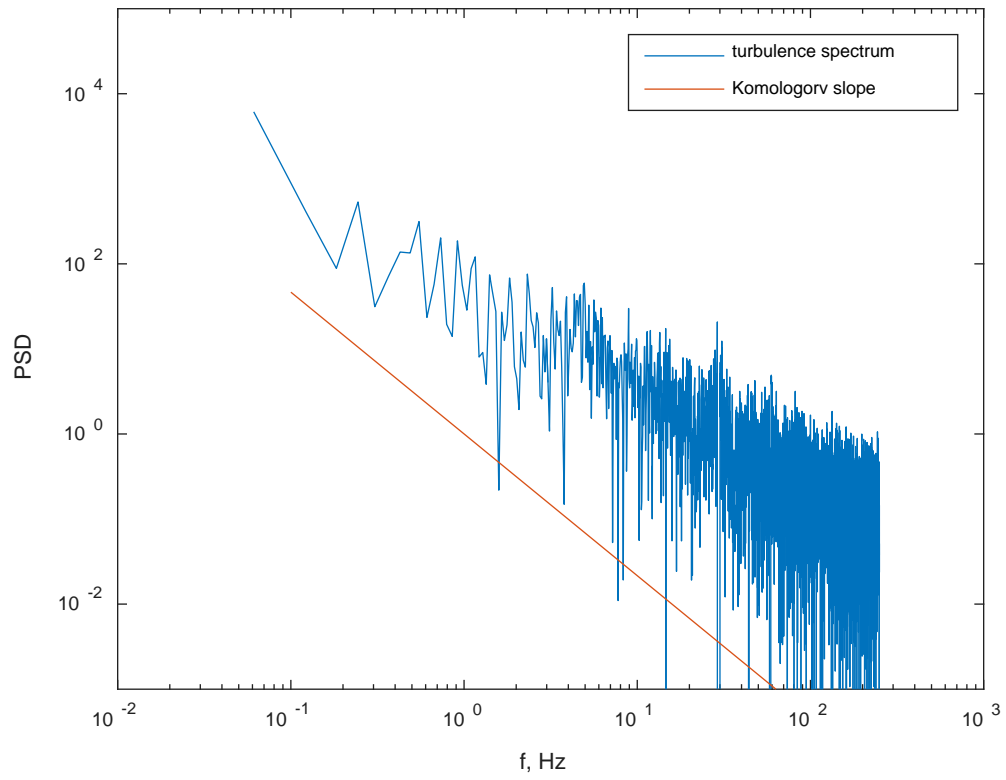


Figure 16: The PSD of the v velocity component for the mixed media. The solid line represents the Kolmogorov  $-5/3$  slope



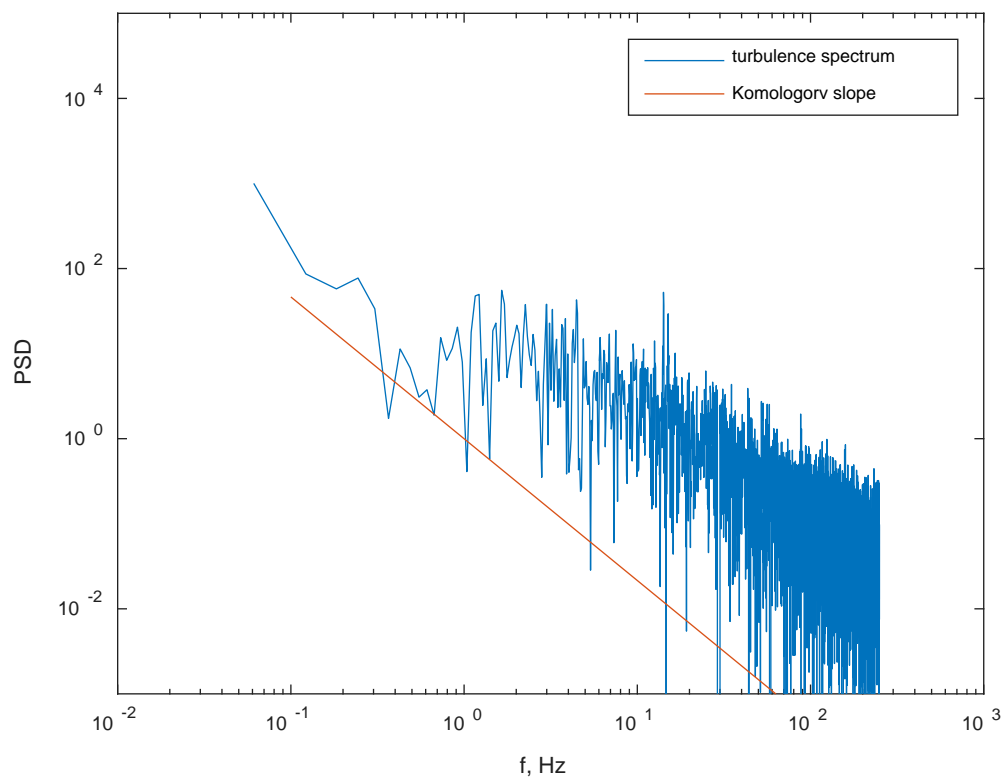


Figure 17: The PSD of the u velocity component for the mixed media. The solid line represents the Kolmogorov  $-5/3$  slope

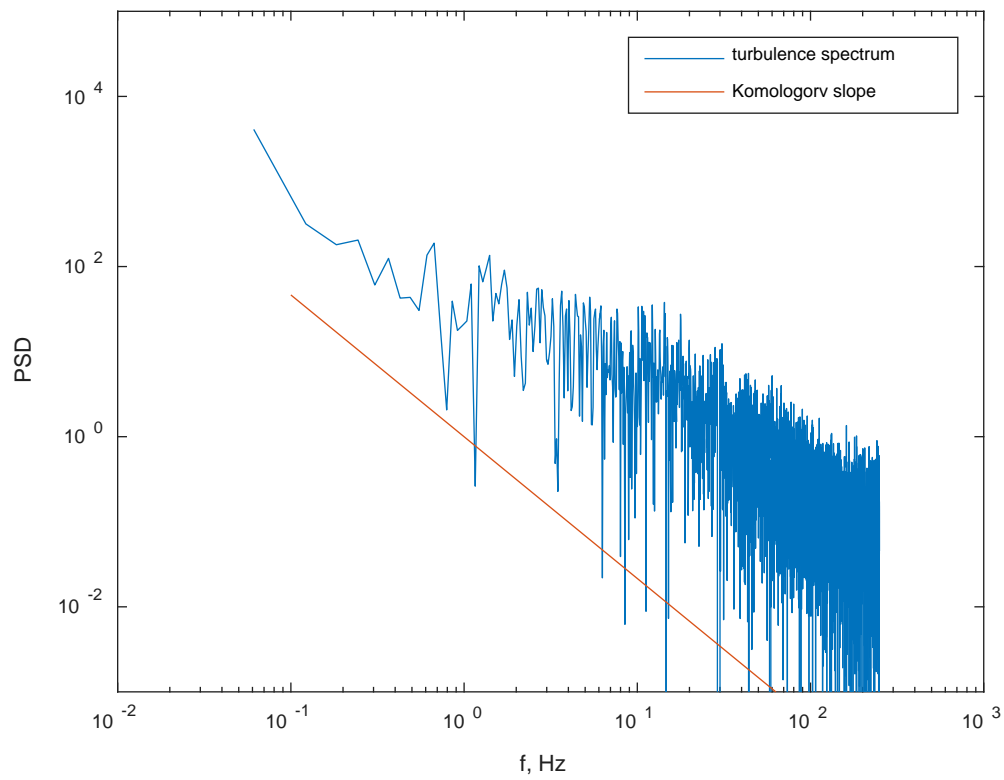


Figure 18: The PSD of the v velocity component for the RS 1022 ZS media. The solid line represents the Kolmogorov  $-5/3$  slope

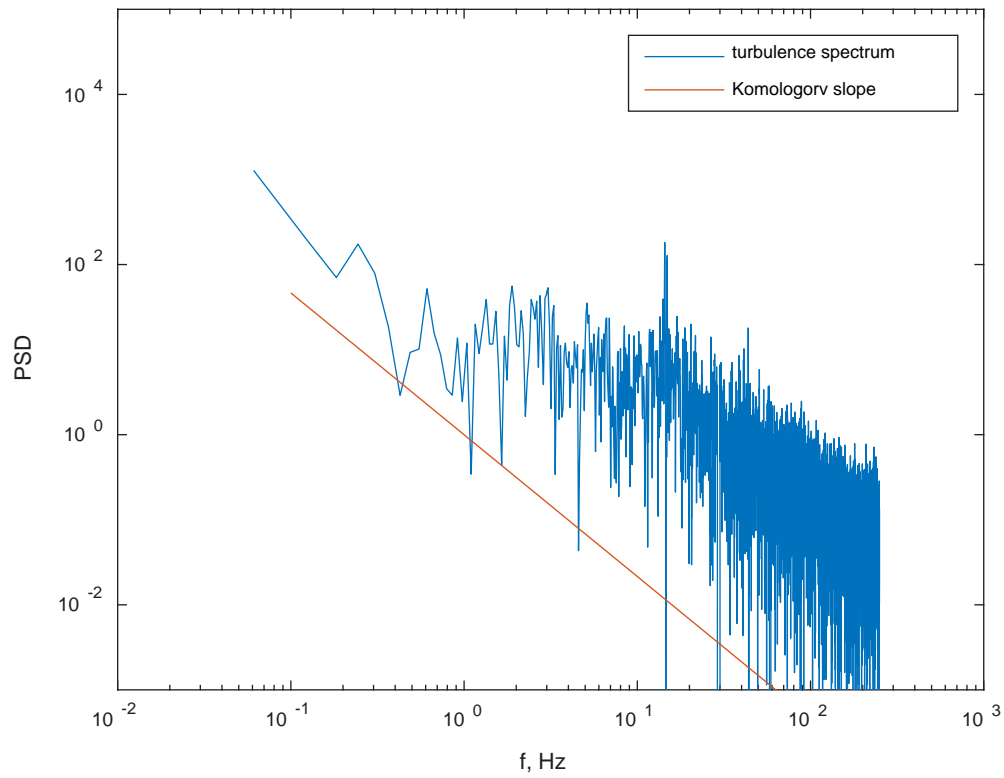


Figure 19: The PSD of the u velocity component for the RS 1022 ZS media. The solid line represents the Kolmogorov  $-5/3$  slope

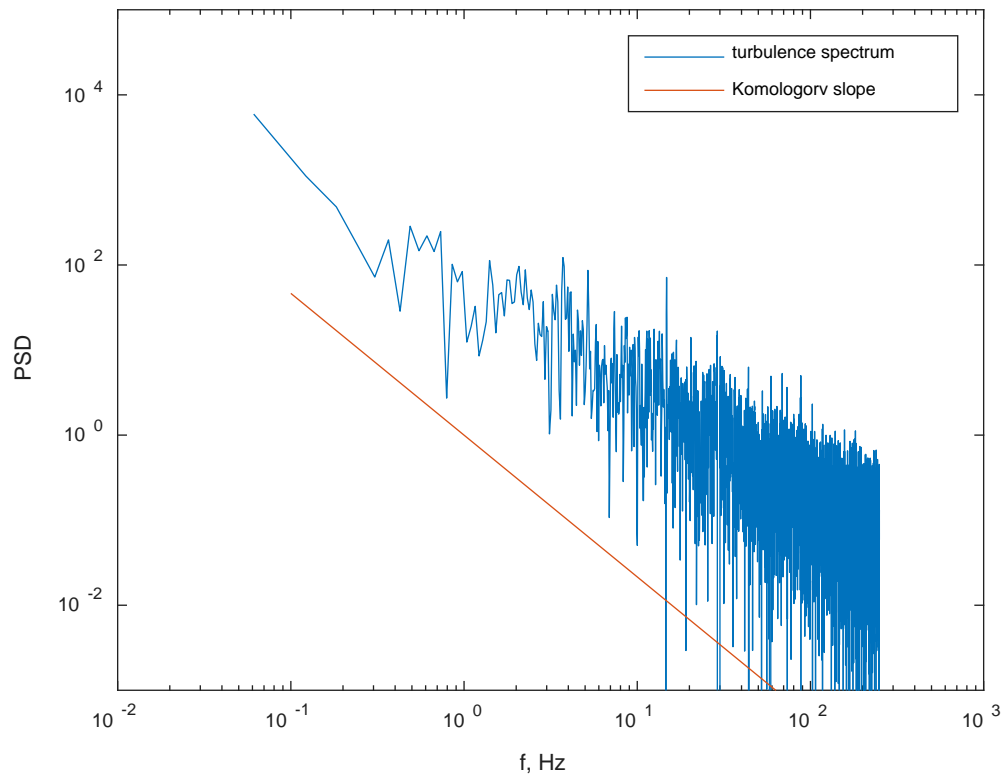


Figure 20: The PSD of the v velocity component for the RSG 10/10 S media. The solid line represents the Kolmogorov  $-5/3$  slope

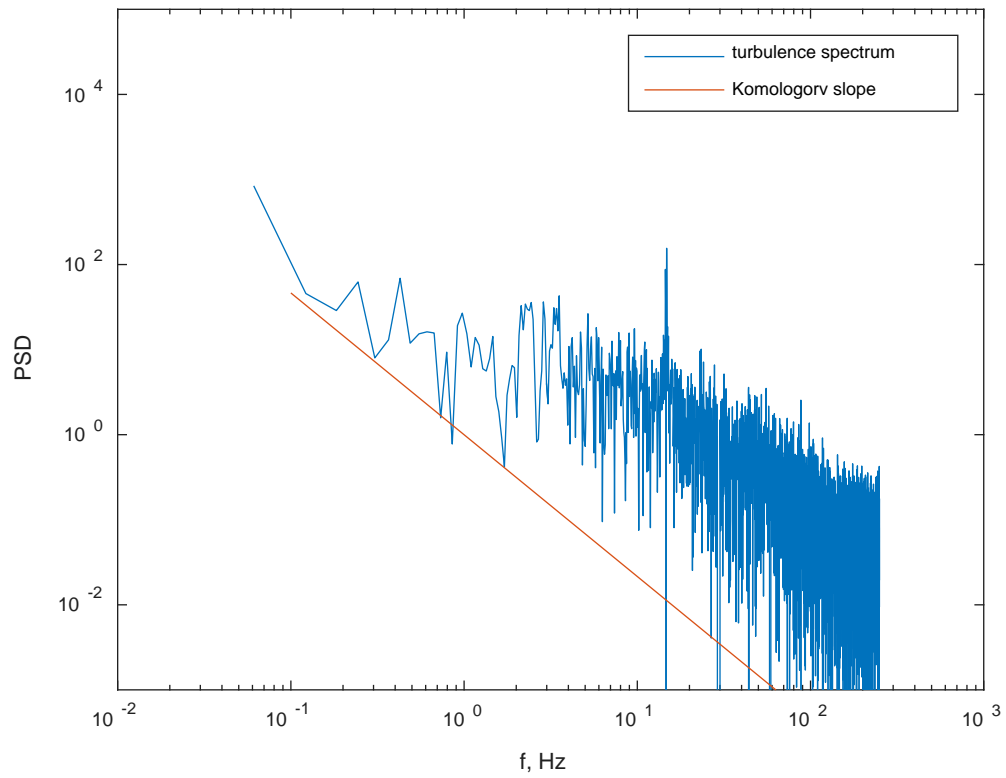


Figure 21: The PSD of the u velocity component for the RSG 10/10 S media. The solid line represents the Kolmogorov  $-5/3$  slope

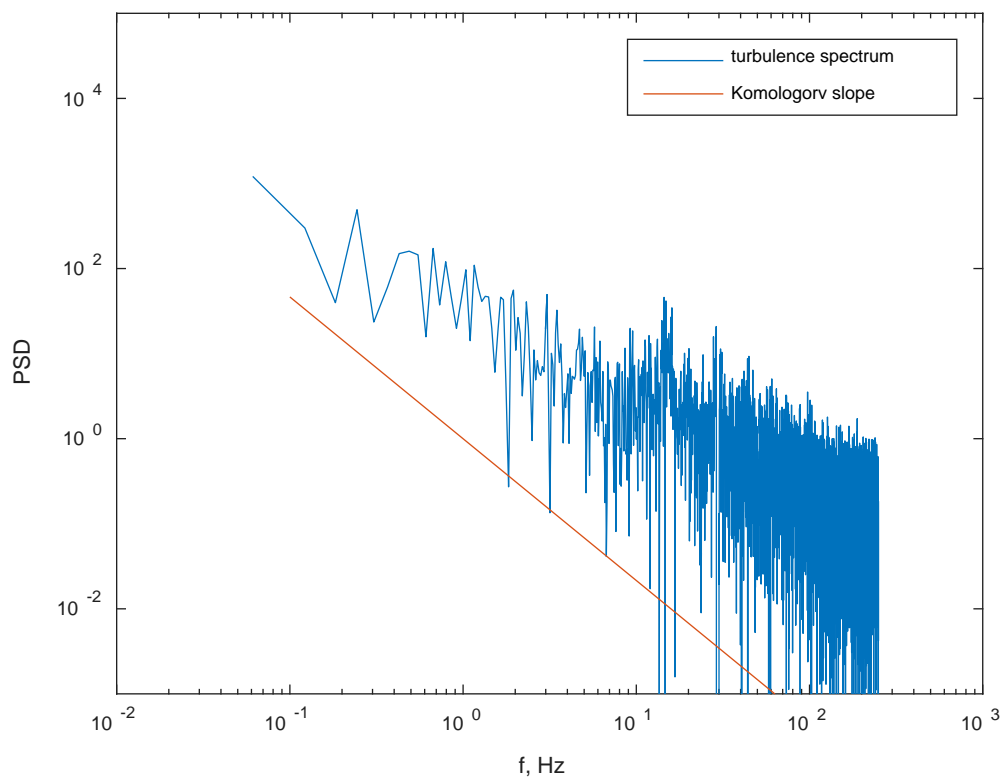


Figure 22: The PSD of the  $v$  velocity component for the RS 35/15 DZS media. The solid line represents the Kolmogorov  $-5/3$  slope

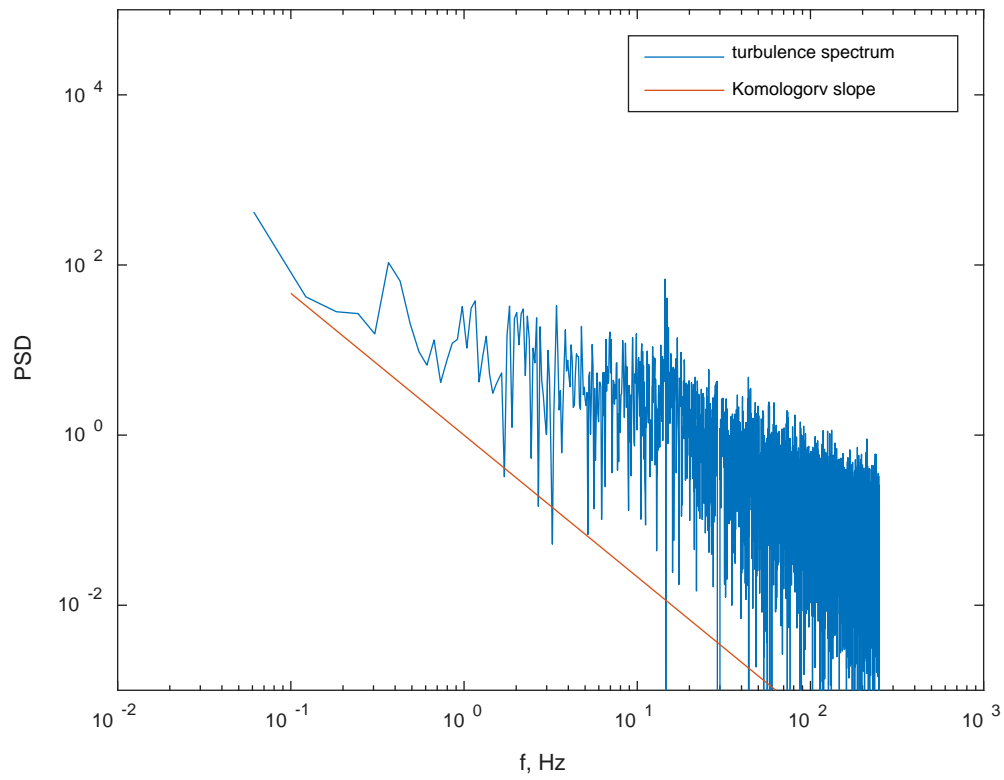


Figure 23: The PSD of the u velocity component for the RS 35/15 DZS media. The solid line represents the Kolmogorov  $-5/3$  slope

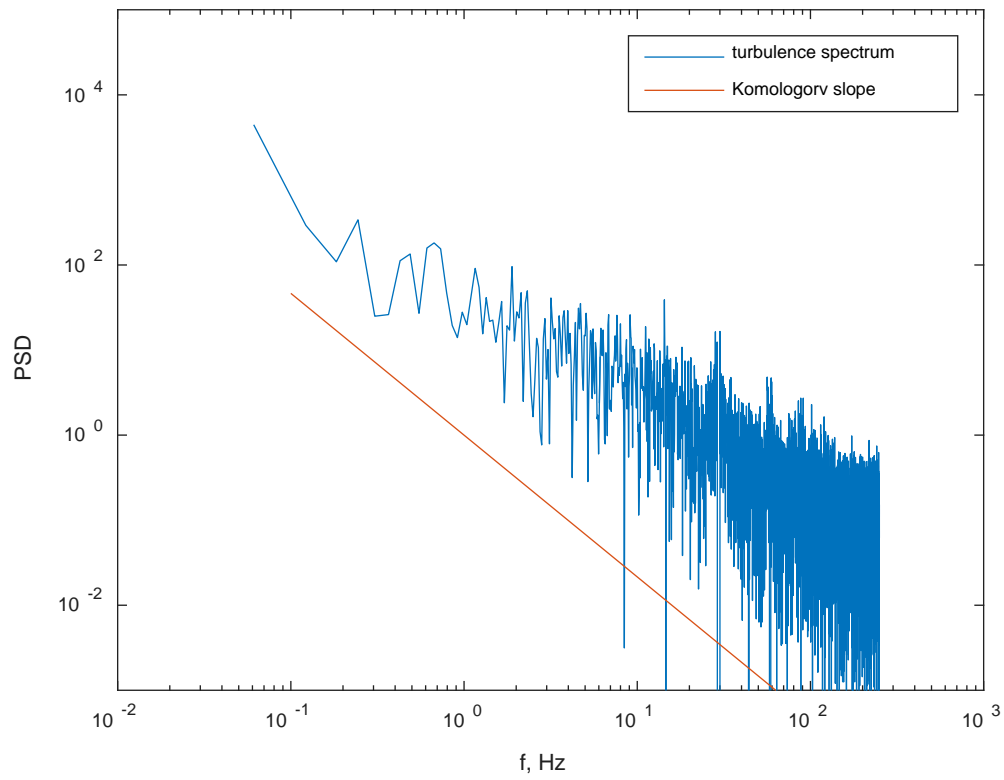


Figure 24: The PSD of the v velocity component for the RS 10/10 media. The solid line represents the Kolmogorov  $-5/3$  slope



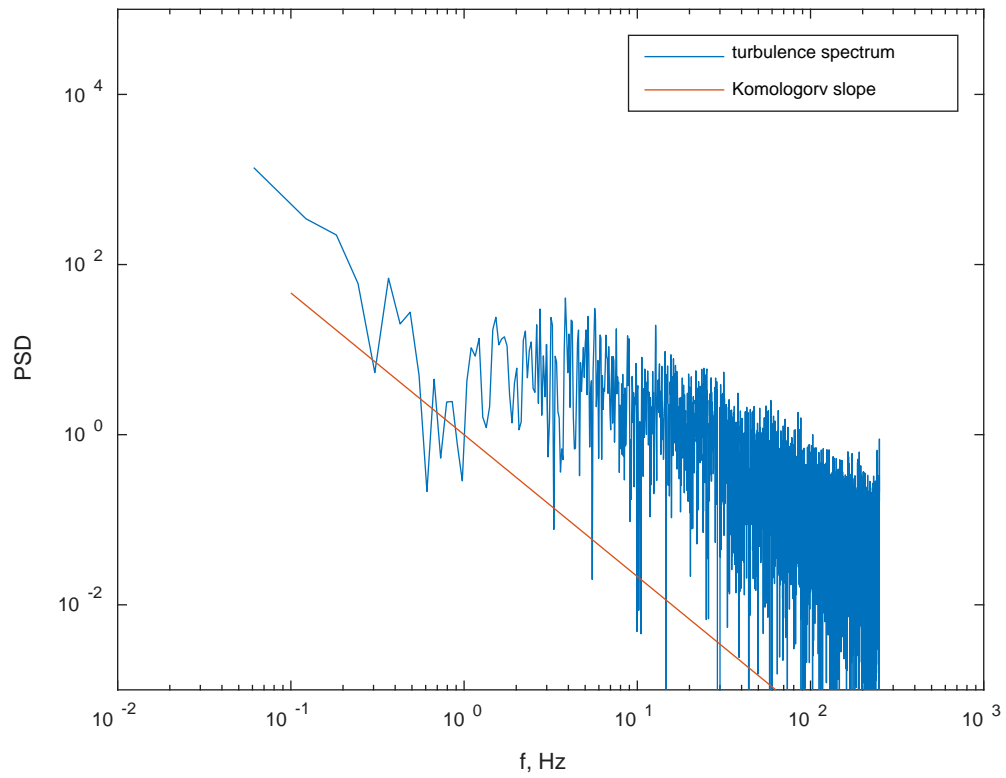


Figure 25: The PSD of the u velocity component for the RS 10/10 media. The solid line represents the Kolmogorov  $-5/3$  slope

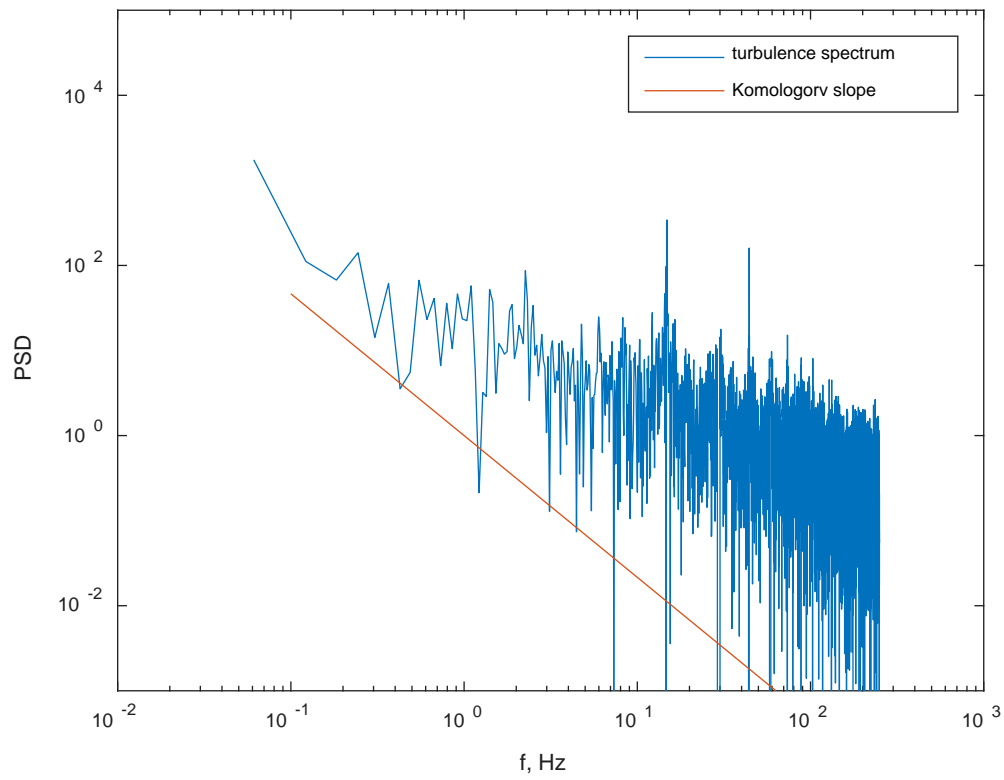


Figure 26: The PSD of the v velocity component for the 2050 40/13 DZ media. The solid line represents the Kolmogorov  $-5/3$  slope

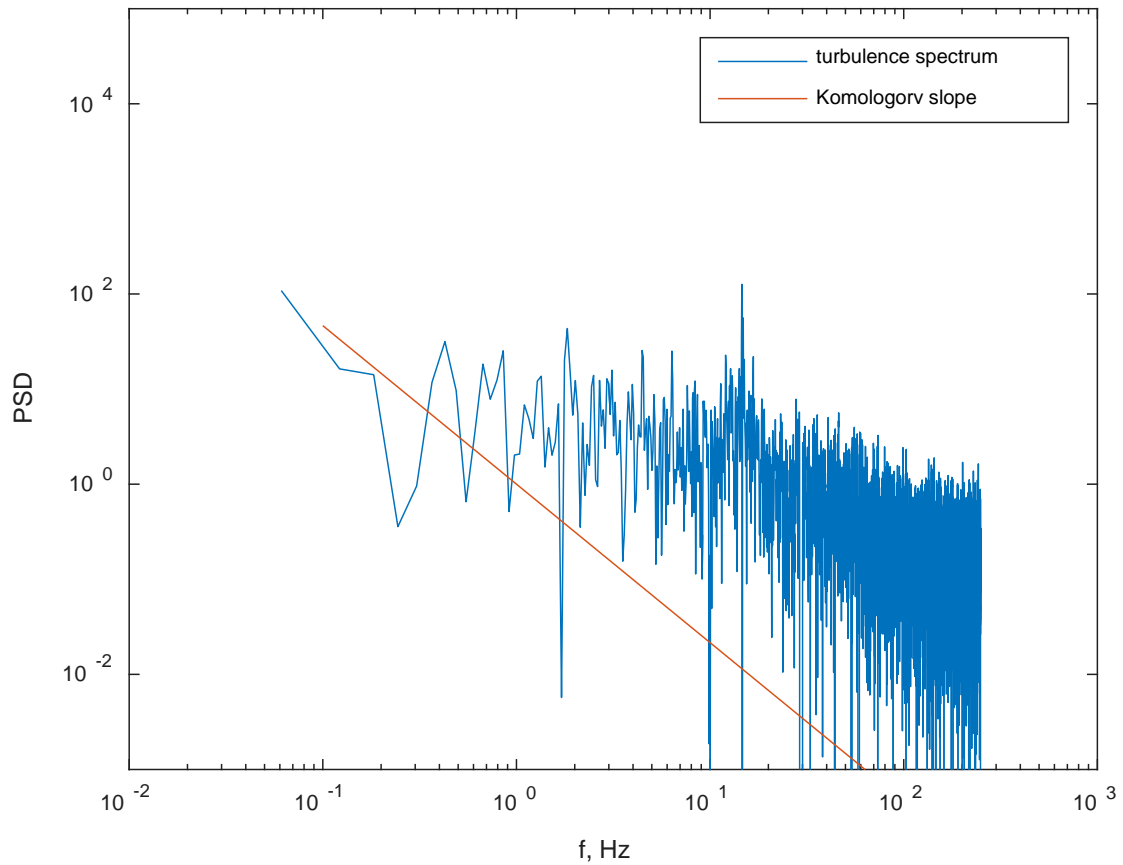


Figure 27: The PSD of the  $u$  velocity component for the 2050 40/13 DZ media. The solid line represents the Kolmogorov  $-5/3$  slope

From the results presented in Figures 6 through 27, the granular turbulence spectra obtained in the study resembled the Kolmogorov spectrum, with both velocity components decreasing as the vortices in the flow became smaller. These findings indicate the presence of an overall decay in the kinetic energy in intermediate scale motion resembling the kinetic energy decay observed in turbulent molecular liquids.

From the turbulence spectra obtained under higher vibrational amplitude presented in Figures 12 and 13, it can be seen that the inertial subrange expanded relative to the inertial subrange observed under lower vibrational amplitudes. This inertial subrange expansion is similar to the behavior observed in turbulent molecular liquids under increased driving amplitudes.

## CHAPTER 7: CONCLUSIONS

From the results obtained in this study, the turbulence spectra show that the granular media flows analyzed exhibit similar vortex breakdown and energy dissipation to what is normally observed in the turbulent flow of molecular liquids, therefore demonstrating that densely packed granular media behave similarly to molecular liquids when undergoing turbulent flow conditions.

In the case of the 2mm spherical grain media for which higher vibrational amplitude measurements were obtained, the inertial subrange expanded under higher amplitudes of vibration relative to the resulting inertial subrange under lower vibrational amplitudes. This inertial subrange expansion under higher driving amplitude is similar to the behavior observed in the turbulent flow of molecular liquids.

The obtained turbulence spectra, along with the higher vibrational amplitude measurements depicting the expansion of the inertial subrange provide strong evidence to support the hypothesis that the observable random grain dynamics in densely packed grain media are equivalent to the unobservable random molecular dynamics present in the flow of molecular liquids.

## REFERENCES

- [1] Fleischhauer, E., Azimi, F., Tkacik, P., Keanini, R., & Mullany, B. (2016). Application of particle image velocimetry (PIV) to vibrational finishing. *Journal of Materials Processing Technology*, 229, 322-328.
- [2] Puglisi, A. (2015). Granular Fluids: From Everyday Life to the Lab. In *Transport and Fluctuations in Granular Fluids* (pp. 1–18). Springer International Publishing. [https://doi.org/10.1007/978-3-319-10286-3\\_1](https://doi.org/10.1007/978-3-319-10286-3_1)
- [3] Puglisi, A. (2015a). Boltzmann Equation: A Gas of Grains. In *Transport and Fluctuations in Granular Fluids* (pp. 19–52). Springer International Publishing. [https://doi.org/10.1007/978-3-319-10286-3\\_2](https://doi.org/10.1007/978-3-319-10286-3_2)
- [4] Puglisi, A. (2015b). Hydrodynamics: A Sea of Grains. In *Transport and Fluctuations in Granular Fluids* (pp. 53–80). Springer International Publishing. [https://doi.org/10.1007/978-3-319-10286-3\\_3](https://doi.org/10.1007/978-3-319-10286-3_3)
- [5] Khusnutdinova, K. (1995). Kolmogorov's 5/3 law. URL: [http://homepages.lboro.ac.uk/~makk/mathrev\\_kolmogorov.pdf](http://homepages.lboro.ac.uk/~makk/mathrev_kolmogorov.pdf). Accessed on April 25, 2017
- [6] Bakker, A. (2002). "Lecture 9-Kolmogorov's Theory". From: Computational Fluid Dynamics course at Dartmouth College. URL: <http://www.bakker.org/dartmouth06/engs150/09-kolm.pdf>. Accessed on April 25, 2017
- [7] Kolesnichenko, I., Pavlinov, A., Golbraikh, E., Frick, P., Kapusta, A., & Mikhailovich, B. (2015). The study of turbulence in MHD flow generated by rotating and traveling magnetic fields. *Experiments in Fluids*, 56(5), 88.
- [8] Karrenberg, U. (2013). Signals in the time and frequency domain. In *Signals, Processes, and Systems* (pp. 33-64). Springer Berlin Heidelberg. [https://doi.org/10.1007/978-3-642-38053-2\\_2](https://doi.org/10.1007/978-3-642-38053-2_2)
- [9] Power Spectral Density Estimates Using FFT - MATLAB & Simulink. MathWorks. URL: <https://www.mathworks.com/help/signal/ug/power-spectral-density-estimates-using-fft.html>. Accessed on: April 25, 2017

- [10] Edge, B. L., & Liu, P. C. (1970). Comparing Power Spectra Computed by Blackman-Tukey and Fast Fourier Transform. *Water Resources Research*, 6(6), 1601-1610.
- [11] Fast Fourier Transform - MATLAB & Simulink. MathWorks. Url: <https://www.mathworks.com/help/matlab/ref/fft.html>. Accessed on: April 25, 2017
- [12] Cerna, M., & Harvey, A. F. (2000). The fundamentals of FFT-based signal analysis and measurement. National Instruments, Application note 4.
- [13] Stiller, J., Koal, K., Nagel, W. E., Pal, J., & Cramer, A. (2013). Liquid metal flows driven by rotating and traveling magnetic fields. *The European Physical Journal Special Topics*, 220(1), 111-122.
- [14] Kareem, W. A., Izawa, S., Xiong, A. K., & Fukunishi, Y. (2009). Lattice Boltzmann simulations of homogeneous isotropic turbulence. *Computers & Mathematics with Applications*, 58(5), 1055-1061.

## APPENDIX A: OVERVIEW OF MATLAB CODE

The MATLAB code used in this study consisted of multiple functions that calculated the velocity in the flow, removed the velocity of the bowl vibration, and calculated the PSD of the velocity components and plotted the turbulence spectrum for each grain type. The different MATLAB files and functions used in this study are included in appendices A through G, along with a brief description of each function.



## APPENDIX B: MAIN FILE

The main body of the code, listed in Appendix B, initiates the command to load the velocity data, and specifies the point in the flow field for which the velocity data should be obtained. After the velocity data are obtained for the specified point, the code uses the various function which will be mentioned shortly to calculate the random velocity in the U and V directions, calculate the PSD of the velocity components at the frequencies present in the flow, and plot the turbulence spectrum for each grain type at the specified location in the flow field.

```

name0909= 'RCP0909_noprobe' ;

nam=strcat(name0909, '.mat' );
load(name0909);

for z = 13;
    for y = 27;

        xpt=z;
        ypt=y;
        freq=30.
        markerbig=3

        [u,v,q,m]=raw2uvqm( Input ,xpt ,ypt );

        [L,NFFT,f,t]=fft_setup( Input );

        U=fft(u)/L;
        V=fft(v)/L;

        Ubowl=bowlonly1(U,f);
        Vbowl=bowlonly1(V,f);

        U2=vibrationremove1(U,f);
        V2=vibrationremove1(V,f);

        u2 = ifft(U2, 'symmetric') *L;
        v2 = ifft(V2, 'symmetric') *L;
        ubowl = ifft(Ubowl, 'symmetric') *L;

```

```

vbw1 = ifft(Vbw1, 'symmetric')*L;

u2avg=mean(u2);
v2avg=mean(v2);
dimu=length(u2);

fil_u=u2(1:dimu);
fil_v=v2(1:dimu);

uavg=mean(fil_u);
vavg=mean(fil_v);

randomu=fil_u-uavg;
randomv=fil_v-vavg;

u_vel = fft(randomu);

y=randomv;
x=randomu;

for i=1:dimu;
    fac1=x(i)*x(i);
    fac2=y(i)*y(i);
    mv(i)=sqrt(fac1+fac2);
end;

maxlag=500;

[acf,lag]=autocorr(mv,maxlag);

tcol=1./freq;
tsamp=0.002;
fac=tsamp/tcol;

```

```

tstar=lag*fac;

X0 = t;
Y0 = randomu;

[freq0 PSD0 nom0]= psd(X0,Y0);

% % % plot command

W = freq0;
A = smooth(PSD0);
AA = smooth(A);
figure(1);pl=psdp(W,PSD0,nom0);
title('RCP 0909');
xlabel('f, Hz');
ylabel('PSD');
legend('turbulence spectrum', 'Komologorv slope');

end
end

namemm= 'MixedMedia_noprobe';

nam=strcat(namemm, '.mat');
load(namemm);

for z = 13;
    for y = 27;
        xpt=z;
        ypt=y;

```

```

[u, v, q, m]=raw2uvqm(Input, xpt, ypt);

[L, NFFT, f, t]=fft_setup(Input);

U=fft(u, NFFT)/L;
V=fft(v, NFFT)/L;

Ubw1=bwonly1(U, f);
Vbw1=bwonly1(V, f);

U2=vibrationremove1(U, f);
V2=vibrationremove1(V, f);

u2 = ifft(U2, NFFT, 'symmetric')*L;
v2 = ifft(V2, NFFT, 'symmetric')*L;
ubow1 = ifft(Ubw1, NFFT, 'symmetric')*L;
vbow1 = ifft(Vbw1, NFFT, 'symmetric')*L;

u2avg=mean(u2);
v2avg=mean(v2);
dimu=length(u2);

fil_u=u2(1:dimu);
fil_v=v2(1:dimu);

uavg=mean(fil_u);
vavg=mean(fil_v);

randomu=fil_u-uavg;
randomv=fil_v-vavg;

y=randomv;
x=randomu;

for i=1:dimu;

```

```

fac1=x(i)*x(i);
fac2=y(i)*y(i);
mv(i)=sqrt(fac1+fac2);
end;

[acf,lag]=autocorr(mv,maxlag);

tcol=1./freq;
tsamp=0.002;
fac=tsamp/tcol;

tstar=lag*fac;

X0 = t;
Y0 = randomu;

[freq0 PSD0 nom0]= psd(X0,Y0);

% % plot command

W = freq0;
A = smooth(PSD0);
AA = smooth(A);
figure(2);pl=psdp(W,PSD0,nom0);
title('mixed media');
xlabel('f, Hz');
ylabel('PSD');
legend('turbulence spectrum','Komologorv slope');
end
end

name1010='RS1010_noprobe';

nam=strcat(name1010, '.mat');
load(name1010);

```

```

for z = 13;
    for y = 27;
        xpt=z;
        ypt=y;
        [u,v,q,m]=raw2uvqm(Input,xpt,ypt);

        [L,NFFT,f,t]=fft_setup(Input);

        U=fft(u,NFFT)/L;
        V=fft(v,NFFT)/L;

        Ubowl=bowlonly1(U,f);
        Vbowl=bowlonly1(V,f);

        U2=vibrationremove1(U,f);
        V2=vibrationremove1(V,f);

        u2 = ifft(U2,NFFT,'symmetric')*L;
        v2 = ifft(V2,NFFT,'symmetric')*L;
        ubowl = ifft(Ubowl,NFFT,'symmetric')*L;
        vbowl = ifft(Vbowl,NFFT,'symmetric')*L;

        u2avg=mean(u2);
        v2avg=mean(v2);
        dimu=length(u2);

        fil_u=u2(1:dimu);
        fil_v=v2(1:dimu);

        uavg=mean(fil_u);
        vavg=mean(fil_v);

        randomu=fil_u-uavg;

```

```

randommv=fil_v-vavg;

y=randomv;
x=randomu;

for i=1:dimu;
    fac1=x(i)*x(i);
    fac2=y(i)*y(i);
    mv(i)=sqrt(fac1+fac2);
end;

[acf,lag]=autocorr(mv,maxlag);

tcol=1./freq;
tsamp=0.002;
fac=tsamp/tcol;

tstar=lag*fac;

X0 = t;
Y0 = randomu;

[freq0 PSD0 nom0]= psd(X0,Y0);

% % plot command

W = freq0;
A = smooth(PSD0);
AA = smooth(A);
figure(3);pl=psdp(W,PSD0,nom0);
title('RS1010');
xlabel('f, Hz');
ylabel('PSD');
legend('turbulence spectrum','Komologorv slope');
end
end

```



```

name3515='RS3515DZS_noprobe';
nam=strcat(name3515, '.mat');
load(name3515);
for z = 13;
    for y = 27;
        xpt=z;
        ypt=y;
        [u,v,q,m]=raw2uvqm(Input,xpt,ypt);
        [L,NFFT,f,t]=fft_setup(Input);
        U=fft(u,NFFT)/L;
        V=fft(v,NFFT)/L;
        Ubowl=bowlonly1(U,f);
        Vbowl=bowlonly1(V,f);
        U2=vibrationremove1(U,f);
        V2=vibrationremove1(V,f);
        u2 = ifft(U2,NFFT,'symmetric')*L;
        v2 = ifft(V2,NFFT,'symmetric')*L;
        ubowl = ifft(Ubowl,NFFT,'symmetric')*L;
        vbowl = ifft(Vbowl,NFFT,'symmetric')*L;
        u2avg=mean(u2);
        v2avg=mean(v2);
        dimu=length(u2);
        fil_u=u2(1:dimu);
        fil_v=v2(1:dimu);

```

```

uavg=mean(fil_u);
vavg=mean(fil_v);

randomu=fil_u-uavg;
randomv=fil_v-vavg;

y=randomv;
x=randomu;

for i=1:dimu;
    fac1=x(i)*x(i);
    fac2=y(i)*y(i);
    mv(i)=sqrt(fac1+fac2);
end;

[acf,lag]=autocorr(mv,maxlag);

tcol=1./freq;
tsamp=0.002;
fac=tsamp/tcol;

tstar=lag*fac;

X0 = t;
Y0 = randomu;

[freq0 PSD0 nom0]= psd(X0,Y0);

% % % plot command

W = freq0;
A = smooth(PSD0);
AA = smooth(A);
figure(4);pl=psdp(W,PSD0,nom0);

```

```

title('RS3515DZS');
xlabel('f, Hz');
ylabel('PSD');
legend('turbulence spectrum', 'Komologorv slope');
end

name19k='RS19K_noprobe';

nam=strcat(name19k, '.mat');
load(name19k);

% set probe point

% original point = xpt=13, ypt=27
for z = 13;
    for y = 27;

xpt=z;
ypt=y;
freq=30.;

[u, v, q, m]=raw2uvqm(Input, xpt, ypt);

[L, NFFT, f, t]=fft_setup(Input);

U=fft(u, NFFT)/L;
V=fft(v, NFFT)/L;

Ubowl=bowlonly1(U, f);
Vbowl=bowlonly1(V, f);

U2=vibrationremove1(U, f);
V2=vibrationremove1(V, f);

```

```

u2 = ifft(U2,NFFT, 'symmetric')*L;
v2 = ifft(V2,NFFT, 'symmetric')*L;
ubowl = ifft(Ubowl,NFFT, 'symmetric')*L;
vbowl = ifft(Vbowl,NFFT, 'symmetric')*L;

u2avg=mean(u2);
v2avg=mean(v2);
dimu=length(u2);

fil_u=u2(1:dimu);
fil_v=v2(1:dimu);

uavg=mean(fil_u);
vavg=mean(fil_v);

randomu=fil_u-uavg;
randomv=fil_v-vavg;

y=randomv;
x=randomu;

for i=1:dimu;
fac1=x(i)*x(i);
fac2=y(i)*y(i);
mv(i)=sqrt(fac1+fac2);
end;

[acf, lag]=autocorr(mv, maxlag);

tcol=1./freq;
tsamp=0.002;
fac=tsamp/tcol;

tstar=lag*fac;

```

```

X0 = t;
Y0 = randomu;

[freq0 PSD0 nom0]= psd(X0,Y0);
% % plot command

W = freq0;
A = smooth(PSD0);
AA = smooth(A);
figure(5);pl=psdp(W,PSD0,nom0);
title('RS19k');
xlabel('f, Hz');
ylabel('PSD');
legend('turbulence spectrum','Komologorv slope');
end

name205='2050_4013DZ_noprobe';

nam=strcat(name205,'.mat');
load(name205);

for z = 13;
    for y = 27;

        xpt=z;
        Ypt=y;
        freq=30.;

        [u,v,q,m]=raw2uvqm(Input,xpt,Ypt);

        [L,NFFT,f,t]=fft_setup(Input);

        U=fft(u,NFFT)/L;
        V=fft(v,NFFT)/L;

```

```

Ubowl=bowlonly1(U,f);
Vbowl=bowlonly1(V,f);

U2=vibrationremove1(U,f);
V2=vibrationremove1(V,f);

u2 = ifft(U2,NFFT, 'symmetric')*L;
v2 = ifft(V2,NFFT, 'symmetric')*L;
ubowl = ifft(Ubowl,NFFT, 'symmetric')*L;
vbowl = ifft(Vbowl,NFFT, 'symmetric')*L;

u2avg=mean(u2);
v2avg=mean(v2);
dimu=length(u2);

fil_u=u2(1:dimu);
fil_v=v2(1:dimu);

uavg=mean(fil_u);
vavg=mean(fil_v);

randomu=fil_u-uavg;
randomv=fil_v-vavg;

y=randomv;
x=randomu;

for i=1:dimu;
    fac1=x(i)*x(i);
    fac2=y(i)*y(i);
    mv(i)=sqrt(fac1+fac2);
end;

[acf,lag]=autocorr(mv,maxlag);

```

```

tcol=1./freq;
tsamp=0.002;
fac=tsamp/tcol;

tstar=lag*fac;

X0 = t;
Y0 = randomu;

[freq0 PSD0 nom0]= psd(X0,Y0);
% % % plot command

W = freq0;
A = smooth(PSD0);
AA = smooth(A);
figure(6);pl=psdp(W,PSD0,nom0);
title('2050');
xlabel('f, Hz');
ylabel('PSD');
legend('turbulence spectrum','Komologorv slope');
end

nameH10='H1008D_noprobe';

nam=strcat(nameH10, '.mat');
load(nameH10);

for z = 13;
    for y = 27;

xpt=z;
Ypt=y;
freq=30.;

```

```

[u,v,q,m]=raw2uvqm(Input,xpt,ypt);
[L,NFFT,f,t]=fft_setup(Input);
U=fft(u,NFFT)/L;
V=fft(v,NFFT)/L;
Ubw1=bwlonly1(U,f);
Vbw1=bwlonly1(V,f);
U2=vibrationremove1(U,f);
V2=vibrationremove1(V,f);
u2 = ifft(U2,NFFT,'symmetric')*L;
v2 = ifft(V2,NFFT,'symmetric')*L;
ubw1 = ifft(Ubw1,NFFT,'symmetric')*L;
vbw1 = ifft(Vbw1,NFFT,'symmetric')*L;
u2avg=mean(u2);
v2avg=mean(v2);
dimu=length(u2);
fil_u=u2(1:dimu);
fil_v=v2(1:dimu);
uavg=mean(fil_u);
vavg=mean(fil_v);
randomu=fil_u-uavg;
randomv=fil_v-vavg;
Y=randomv;
x=randomu;

```



```

for i=1:dimu;
    fac1=x(i)*x(i);
    fac2=y(i)*y(i);
    mv(i)=sqrt(fac1+fac2);
end;

[acf,lag]=autocorr(mv,maxlag);

tcol=1./freq;
tsamp=0.002;
fac=tsamp/tcol;

tstar=lag*fac;

X0 = t;
Y0 = randomu;

[freq0 PSD0 nom0]= psd(X0,Y0);
% % plot command

W = freq0;
A = smooth(PSD0);
AA = smooth(A);
figure(7);pl=psdp(W,PSD0,nom0);
title('H10');
xlabel('f, Hz');
ylabel('PSD');
legend('turbulence spectrum', 'Komologorv slope');
end

nameRSG1010='RSG1010S_noprobe';

nam=strcat(nameRSG1010, '.mat');
load(nameRSG1010);

```

```

for z = 13;
    for Y = 27;

        xpt=z;
        Ypt=Y;
        freq=30.;

        [u,v,q,m]=raw2uvqm(Input,xpt,Ypt);

        [L,NFFT,f,t]=fft_setup(Input);

        U=fft(u,NFFT)/L;
        V=fft(v,NFFT)/L;

        Ubowl=bowlonly1(U,f);
        Vbowl=bowlonly1(V,f);

        U2=vibrationremove1(U,f);
        V2=vibrationremove1(V,f);

        u2 = ifft(U2,NFFT,'symmetric')*L;
        v2 = ifft(V2,NFFT,'symmetric')*L;
        ubowl = ifft(Ubowl,NFFT,'symmetric')*L;
        vbowl = ifft(Vbowl,NFFT,'symmetric')*L;

        u2avg=mean(u2);
        v2avg=mean(v2);
        dimu=length(u2);

        fil_u=u2(1:dimu);
        fil_v=v2(1:dimu);

        uavg=mean(fil_u);
        vavg=mean(fil_v);

```

```

randomu=fil_u-uavg;
randomv=fil_v-vavg;

y=randomv;
x=randomu;

for i=1:dimu;
    fac1=x(i)*x(i);
    fac2=y(i)*y(i);
    mv(i)=sqrt(fac1+fac2);
end;

[acf, lag]=autocorr(mv, maxlag);

tcol=1./freq;
tsamp=0.002;
fac=tsamp/tcol;

tstar=lag*fac;

X0 = t;
Y0 = randomu;

[freq0 PSD0 nom0]= psd(X0, Y0);
% % plot command

W = freq0;
A = smooth(PSD0);
AA = smooth(A);
figure(8);pl=psdp(W, PSD0, nom0);
title('RSG1010');
xlabel('f, Hz');
ylabel('PSD');
legend('turbulence spectrum', 'Komologorv slope');
end

```

```

end

nameRS3515='RS3515DZS_noprobe';

nam=strcat(nameRS3515, '.mat');
load(nameRS3515);

for z = 13;
    for y = 27;

        xpt=z;
        Ypt=y;
        freq=30.;

        [u,v,q,m]=raw2uvqm(Input,xpt,Ypt);

        [L,NFFT,f,t]=fft_setup(Input);

        U=fft(u,NFFT)/L;
        V=fft(v,NFFT)/L;

        Ubowl=bowlonly1(U,f);
        Vbowl=bowlonly1(V,f);

        U2=vibrationremove1(U,f);
        V2=vibrationremove1(V,f);

        u2 = ifft(U2,NFFT,'symmetric')*L;
        v2 = ifft(V2,NFFT,'symmetric')*L;
        ubowl = ifft(Ubowl,NFFT,'symmetric')*L;
        vbowl = ifft(Vbowl,NFFT,'symmetric')*L;

        u2avg=mean(u2);
        v2avg=mean(v2);

```

```

dimu=length(u2);
fil_u=u2(1:dimu);
fil_v=v2(1:dimu);
uavg=mean(fil_u);
vavg=mean(fil_v);
randomu=fil_u-uavg;
randomv=fil_v-vavg;
y=randomv;
x=randomu;
for i=1:dimu;
fac1=x(i)*x(i);
fac2=y(i)*y(i);
mv(i)=sqrt(fac1+fac2);
end;
[acf,lag]=autocorr(mv,maxlag);
tcol=1./freq;
tsamp=0.002;
fac=tsamp/tcol;
tstar=lag*fac;
X0 = t;
Y0 = randomu;
[freq0 PSD0 nom0]= psd(X0 , Y0 );
% % % plot command
W = freq0;

```

```

A = smooth(PSD0);
AA = smooth(A);
figure(9);pl=psdp(W,PSD0,nom0);
title('RS3515');
xlabel('f, Hz');
ylabel('PSD');
legend('turbulence spectrum', 'Komologorv slope');
end

nameRS1022='RS1022ZS_noprobe';

nam=strcat(nameRS1022, '.mat');
load(nameRS1022);

for z = 13;
    for y = 27;

        xpt=z;
        ypt=y;
        freq=30.;

        [u,v,q,m]=raw2uvqm(Input,xpt,ypt);

        [L,NFFT,f,t]=fft_setup(Input);

        U=fft(u,NFFT)/L;
        V=fft(v,NFFT)/L;

        Ubowl=bowlonly1(U,f);
        Vbowl=bowlonly1(V,f);

        U2=vibrationremove1(U,f);
        V2=vibrationremove1(V,f);

```

```

u2 = ifft(U2,NFFT, 'symmetric')*L;
v2 = ifft(V2,NFFT, 'symmetric')*L;
ubowl = ifft(Ubowl,NFFT, 'symmetric')*L;
vbowl = ifft(Vbowl,NFFT, 'symmetric')*L;

u2avg=mean(u2);
v2avg=mean(v2);
dimu=length(u2);

fil_u=u2(1:dimu);
fil_v=v2(1:dimu);

uavg=mean(fil_u);
vavg=mean(fil_v);

randomu=fil_u-uavg;
randomv=fil_v-vavg;

y=randomv;
x=randomu;

for i=1:dimu;
fac1=x(i)*x(i);
fac2=y(i)*y(i);
mv(i)=sqrt(fac1+fac2);
end;

[acf, lag]=autocorr(mv, maxlag);

tcol=1./freq;
tsamp=0.002;
fac=tsamp/tcol;

tstar=lag*fac;

```

```

X0 = t;
Y0 = randomu;

[freq0 PSD0 nom0]= psd(X0,Y0);
% % plot command

W = freq0;
A = smooth(PSD0);
AA = smooth(A);
figure(10);pl=psdp(W,PSD0,nom0);
title('RS1022');
xlabel('f, Hz');
ylabel('PSD');
legend('turbulence spectrum','Komologorv slope');
end

name2mmsphere='2mmsphere_noprobe';

nam=strcat(name2mmsphere, '.mat');
load(name2mmsphere);

for z = 13;
    for y = 27;

        xpt=z;
        ypt=y;
        freq=30.;

        [u,v,q,m]=raw2uvqm(Input,xpt,ypt);

        [L,NFFT,f,t]=fft_setup(Input);

```



```

U=fft(u,NFFT)/L;
V=fft(v,NFFT)/L;

Ubw1=bwonly1(U,f);
Vbw1=bwonly1(V,f);

U2=vibrationremove1(U,f);
V2=vibrationremove1(V,f);

u2 = ifft(U2,NFFT,'symmetric')*L;
v2 = ifft(V2,NFFT,'symmetric')*L;
ubw1 = ifft(Ubw1,NFFT,'symmetric')*L;
vbw1 = ifft(Vbw1,NFFT,'symmetric')*L;

u2avg=mean(u2);
v2avg=mean(v2);
dimu=length(u2);

fil_u=u2(1:dimu);
fil_v=v2(1:dimu);

uavg=mean(fil_u);
vavg=mean(fil_v);

randomu=fil_u-uavg;
randomv=fil_v-vavg;

y=randomv;
x=randomu;

for i=1:dimu;
    fac1=x(i)*x(i);
    fac2=y(i)*y(i);
    mv(i)=sqrt(fac1+fac2);
end;

```

```
[acf, lag]=autocorr(mv, maxlag);

tcol=1./freq;
tsamp=0.002;
fac=tsamp/tcol;

tstar=lag*fac;

X0 = t;
Y0 = randomu;

[freq0 PSD0 nom0]= psd(X0, Y0);
% % plot command

W = freq0;
A = smooth(PSD0);
AA = smooth(A);
figure(11);pl=psdp(W, PSD0, nom0);
title('2mmSphere');
xlabel('f, Hz');
ylabel('PSD');
legend('turbulence spectrum', 'Komologorv slope');
end
end
```

## APPENDIX C: RAW2UVQM FUNCTION

This function is used to obtain the raw u and v direction velocities calculated through the PIV results.

```
function [u, v, q, m]=raw2uvqm(Input, Y, x)
    for i=1:length(Input{1}.dataset)
        u(i)=Input{1}.dataset(i).U(Y, x); % (Y, x)
        v(i)=Input{1}.dataset(i).V(Y, x);
    end
end
```

## APPENDIX D: FFT\_SETUP FUNCTION

This function obtains the sample time of the data set being analyzed, calculates the frequency, obtains the length of the signal, initiates the time vector, and determines the value of NFFT.

```
function [L,NFFT,f,t]=fft_setup(Input)

T=Input{1}.timeBtwPulses; % sample time
Fs=1/T; % sample frequency
L=length(Input{1}.dataset); % length of signal
NFFT=2^nextpow2(L); % Next power of 2 from length u
t= (0:L-1)*T; % Time vector

f=Fs/2*linspace(0,1,NFFT/2+1);

end
```

## APPENDIX E: VIBRATIONREMOVE FUNCTION

This function is used to remove the U and V velocity components resulting from the vibration of the bowl. The function removes the vibrations of the bowl from the total velocity data by identifying the frequencies of the bowl vibrations and setting them equal to zero, therefore removing the velocity components of the bowl vibrations from the velocity data.

```
function [V2] = vibrationremove1(V,f)
```

```
V2=V;
```

```
V2(f>14.6 & f<14.7)=0;
```

```
V2(f>29.0 & f<30.0)=0;
```

```
V2(f>43.9 & f<44.2)=0;
```

```
V2(f>58.0 & f<59.0)=0;
```

```
V2(f>73.4 & f<73.5)=0;
```

```
V2(f>88.0 & f<88.2)=0;
```

```
V2(f>102.7 & f<102.8)=0;
```

```
V2(f>117.3 & f<117.5)=0;
```

```
V2(f>132.0 & f<132.1)=0;
```

```
V2(f>146.6 & f<146.8)=0;
```

```
V2(f>161.3 & f<161.4)=0;
```

```
V2(f>175.9 & f<176.1)=0;
```

```
V2(f>190.6 & f<190.7)=0;
```

```
V2(f>205.2 & f<205.4)=0;
```



```
V2(f>219.9 & f<220.0)=0;  
V2(f>234.5 & f<234.7)=0;  
V2(f>249.2 & f<249.3)=0;  
end
```

## APPENDIX F: PSD FUNCTION

This function calculates the power spectral density of the U and V velocity components of the flow at the specified location in the flow field, as well as the frequencies present in the flow.

```

function [freq0 PSD0 nom0]=psd(X0,Y0)

%X0 is time in a time domain data
%Y0 is the parameter changing with time (in your case the kinetic energy)

dx = (X0(2)-X0(1))*10^0;
zf0 = fft(Y0*10^3);%implementing the DFT
nom0 = length(Y0);
PSD0 = dx/nom0*(abs(zf0).^2);%calculation of the psd
jj0= (2:1:floor(nom0/2)+1);
freq0 = (jj0-1)/(nom0*dx);%cacluclation of the frequencie

```

## APPENDIX G: PSDP FUNCTION

The PSDP function plots the power spectral density (PSD) of the velocity components against the frequencies in the flow. This function also plots a solid line of a  $(-5/3)$  slope representing the Kolmogorov slope for the inertial subrange.

```
function p1=psdp(W,A,nom0)

p1 = loglog(W,A(2:floor(nom0/2)+1));%plot of the psd and c is the color
ylim([10^-3 10^5]);
hold on

aa = [ 10^-1 10^1 10^2 10^3];
bb = aa.^(-5/3);
loglog(aa,bb)
```